

# THREE-DIMENSIONAL PHOTONIC CRYSTALS MADE FROM COLLOIDS

Arnout Imhof\*

## 1. INTRODUCTION

One of the most fascinating properties of monodisperse colloids is that they can form ordered phases. These phases can be thermodynamically stable if the volume fraction of particles is high enough, or they can form under the influence of an external field such as gravity or an electric field. The particles are small enough to exhibit Brownian motion, which causes them to move around randomly until the collective has found a state of minimal free energy. In a colloidal crystal the (almost always spherical) particles stack regularly to form a long-range, three-dimensional array. Particles shaped like rods or plates form additional liquid crystalline phases with nematic or smectic order. The spontaneous formation of such phases is nowadays often called self-assembly or self-organization. Colloidal crystallization has been studied intensively ever since the time that methods became available to synthesize sufficiently monodisperse colloids, i.e. those with particles having sizes that are uniform to better than about 8%.<sup>1-3</sup> Apart from being interesting for their statistical mechanical behaviour colloidal crystals have special and useful optical properties.

The best-known colloidal crystal with special optical properties is almost certainly the opal. It consists of a three-dimensional array of submicrometer silica spheres, which must have formed naturally in a sediment and then cemented together.<sup>4-6</sup> Visible light diffracts from the lattice planes, just like Bragg diffraction of X-rays from molecular crystals. The result is a beautiful iridescence, earning opals the qualification gemstones. Opals can also be made artificially by sedimenting monodisperse silica spheres in the laboratory, after which they are dried and sintered together.

Diffraction by colloidal crystals has also been recognized as a useful optical property. Thus, Asher and co-workers have put these crystals to use as narrow-band filters, that efficiently reject Rayleigh scattered incident light in Raman spectroscopy,<sup>7</sup> as nanosecond optical switches,<sup>8</sup> and as chemical sensors.<sup>9</sup>

In an independent development certain periodic dielectric structures have been proposed as materials which would not permit the propagation of electromagnetic waves

---

\* Arnout Imhof, Debye Institute, Utrecht University, Postbus 80000, 3508 TA Utrecht, The Netherlands.

in a range of frequencies called the photonic band gap.<sup>10,11</sup> In this respect they are to light what semiconductors are to electrons. Such materials are called photonic crystals. Photonic crystals would inhibit spontaneous emission by excited atoms or molecules embedded inside and would localize light to a small volume around impurities. The first photonic crystal was made by Yablonovitch by drilling three sets of cylindrical holes in a block of dielectric in a periodic arrangement.<sup>12</sup> The periodicity was on the order of a millimeter so that the photonic band gap appeared at microwave frequencies.

Photonic crystals offer unique ways to control the propagation of electromagnetic waves.<sup>13</sup> Crystals possessing a band gap will behave like semiconductors for light, offering the possibility that light may be manipulated in ways similar to the way electrons are controlled by semiconductors. If light is forbidden to propagate through the crystal it would remain trapped at defect sites. Such a defect can be shaped in the form of a tiny cavity or as a sharply-curved waveguide, allowing one to manipulate light in ways that have not been possible before. Thus, photonic crystals have been proposed for a large number of applications such as efficient microwave antennas, zero-threshold lasers, low-loss resonators, optical switches, and miniature optoelectronic components such as microlasers and waveguides. The most useful applications would occur at near-infrared or visible wavelengths. This makes it necessary to fabricate photonic crystals with feature sizes of less than a micrometer. Furthermore, the refractive index contrast of the crystal must exceed 2 or 3, depending on the lattice, placing restrictions on the materials used.

A number of different methods is used for the fabrication of photonic crystals. Many of these apply a variety of lithographic techniques used in the semiconductor industry for patterning substrates such as silicon. Two-dimensional photonic crystals have been made this way, which operate at wavelengths down to the visible.<sup>13</sup> Good control over the introduction of defects has also been demonstrated. A number of attempts has been made to create three-dimensional photonic crystals using these techniques.<sup>14-16</sup> However, it has so far proved too difficult to achieve submicron periodicities of much more than one unit cell thickness.

On the other hand, colloidal particles naturally possess the desired sizes and can form periodic structures spontaneously. Moreover, the optical properties of the individual spheres can easily be tuned, or they can be used as templates to make inverted structures. Colloids have therefore been proposed as an easy and inexpensive way to fabricate three-dimensional photonic crystals, and as a suitable system in which to investigate their optical properties.<sup>17,18</sup> Until this realization colloidal crystals had been prepared with only a modest refractive index contrast, in order for them to remain relatively transparent and not opaque due to multiple scattering. They can thus be said to reject light propagating in certain directions, which satisfy the Bragg condition:

$$2d \sin \theta = m\lambda . \quad (1)$$

Here,  $\lambda$  is the wavelength of the light in the crystal,  $d$  the lattice spacing,  $\theta$  the angle between the incident ray and the lattice planes, and the integer  $m$  is the order of the diffraction. If the dielectric contrast between the spheres and the suspending medium is made larger the range of angles for which waves of a given frequency diffract increases due to multiple scattering. At sufficiently high contrast and for certain crystal types propagation should become impossible in all directions and for both polarizations.

In this chapter, I will describe the fabrication and optical properties of photonic crystals. I will concentrate on the work using colloidal suspensions; however, not without making comparisons with other methods where necessary. Fabrication of photonic crystals is guided by numerical calculation of their optical properties. Therefore, I will start in section 2 with a description of the most important optical properties of photonic crystals, as well as the theories used to describe them and experimental techniques used to probe them. In section 3 methods for the fabrication of photonic crystals are discussed with an emphasis on methods using colloidal self-assembly. Section 4 describes recent work using composite colloids such as core-shell or metallo-dielectric particles.

## 2. OPTICAL PROPERTIES OF PHOTONIC CRYSTALS

Propagation of electromagnetic waves in periodic media displays many interesting and useful effects. It was already described in the theory of X-ray diffraction by solids in the early 20<sup>th</sup> century by Ewald and von Laue, see e.g. refs. 19,20. Materials with a layered structure ('stratified media') are used as high reflectance dielectric mirrors,<sup>21</sup> but also as diffraction gratings, distributed feedback lasers, and acousto-optic filters. Materials with a periodicity in only one dimension are not usually called photonic crystals, nor is this the case for materials in which the variation in refractive index is very small, such as in X-ray diffraction where it is at most  $\sim 10^{-4}$ .

### 2.1. Propagation of Light in Photonic Crystals

Electromagnetic waves propagating in a photonic crystal experience a periodic variation of the refractive index. At every interface part of the incident wave is reflected (or scattered) and the rest is transmitted. Interference between reflected and transmitted waves determines the wave form in the crystal. This wave form has a periodicity corresponding to that of the crystal lattice and can be determined from the Maxwell equations. For a given angular frequency  $\omega$  the solutions of the fields have a periodic wave form and are called Bloch modes:

$$\exp(i\mathbf{k}\cdot\mathbf{r})\mathbf{u}_{\mathbf{k}}(\mathbf{r}). \quad (2)$$

Here,  $\mathbf{u}_{\mathbf{k}}(\mathbf{r})$  is a function with the same periodicity as the crystal. It is labeled with the Bloch wave vector  $\mathbf{k}$ , describing the period and direction of propagation of the wave. The frequencies of the allowed modes  $\omega(\mathbf{k})$  form the so-called dispersion relation. There will in general be frequencies for which solutions exist only in some directions but not in others. These waves cannot propagate in the excluded directions. Physically, this means that destructive interference cancels the wave in those directions. Instead, the wave is reflected. This is analogous to Bragg diffraction as described by Eq. (1). There may even be one or more ranges of frequencies for which there exists no wave form for  $\mathbf{k}$ 's in any direction. Such waves are forbidden to propagate in the crystal. Their frequencies are said to be in the photonic band gap.

In Figure 1 the frequencies of the allowed modes are plotted versus wave vectors in the Brillouin zone of a face-centered cubic lattice of spheres consisting of air in a

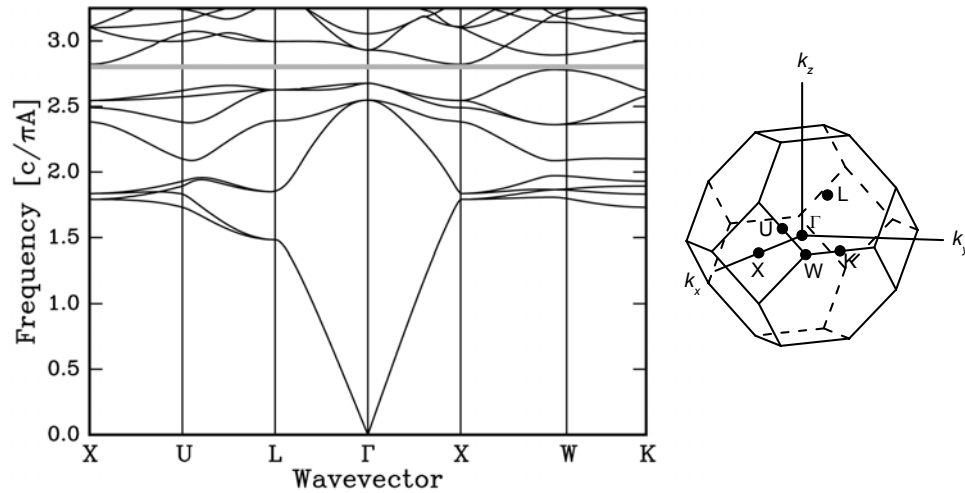


**Figure 1.** (a) Band structure of an ‘inverse’ fcc lattice of spheres of refractive index 1 in a background with index 3 calculated with the KKR method.<sup>22</sup> The horizontal gray band outlines the complete band gap. The letters indicate wave vectors corresponding to the special points of the fcc Brillouin zone shown in (b).

background material of refractive index 3. The allowed modes form the photonic band structure of this crystal. There is a narrow band gap at a frequency of  $\nu = 2.8c/\pi A$ , where  $c$  is the speed of light and  $A$  the size of the cubic unit cell. The ‘inverted’ crystal structure is shown here because the ‘direct’ structure, i.e. spheres of high refractive index in air, does not possess a band gap. If the refractive index contrast (the ratio of the refractive index of the spheres and their background) is increased the band gap widens. Below a contrast of 2.85 the gap is closed.<sup>22</sup>

The band gap in Figure 1 is located between the 8<sup>th</sup> and 9<sup>th</sup> bands. This corresponds to the region where, in weakly scattering crystals, the second order Bragg diffraction is located. The first order Bragg diffraction occurs at a lower frequency, around  $\nu = 1.7c/\pi A$  for the direction corresponding to the L point. At this point the waves travel perpendicularly to the (111) planes of the crystal. There is a sizeable range of frequencies for which these waves cannot propagate in the crystal and thus are reflected. This frequency range is called a stopgap. Since propagation is still possible in other directions one usually speaks of a partial or incomplete band gap. If the direction is moved away from the L or X points the bands are seen to split in two. These are the different polarization states which are then no longer degenerate.

There is a close analogy with electron waves traveling in the periodic potential of atomic crystals. There, too, the allowed modes are arranged into energy bands separated by energy gaps. That is why much of the terminology in the photonic crystal literature is borrowed from solid state physics. There are also important differences, however, most importantly the fact that electrons are described by scalar wave fields, whereas electromagnetic waves are vectorial in nature, describing the two polarizations, which are not independent.

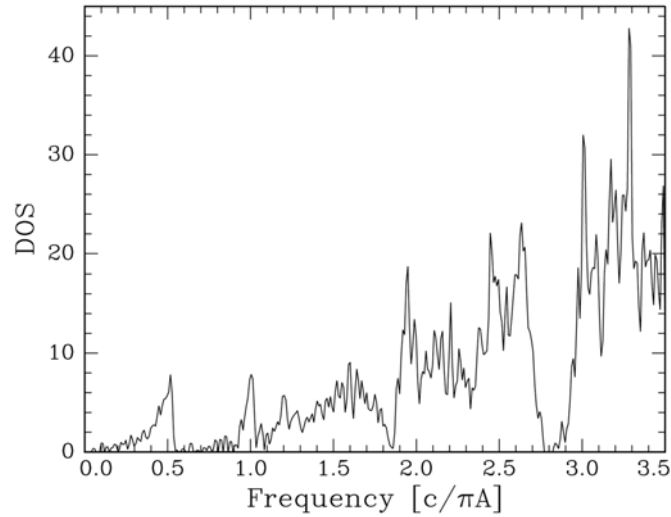


Figure 2. Photonic density of states of the inverse fcc crystal of Figure 1.

Due to the photonic band structure the number of allowed modes varies with frequency. This is described by the density of states (DOS), which is the number of photon modes per unit of frequency. This function is shown in Figure 2 for the fcc crystal of Figure 1. The DOS vanishes for frequencies in the photonic band gap. Around  $\nu = 1.8c/\pi A$  the DOS is strongly depleted, but nonvanishing. This region is usually referred to as a pseudogap. The density of states is important for the emission of an excited atom or molecule, because the decay rate of the latter is proportional to the local density of states (LDOS). The LDOS depends strongly on the position within the unit cell.<sup>23,24</sup> In a complete photonic band gap the excited atom cannot decay radiatively, wherever it is sitting. Ideally, it will remain in its excited state until it decays nonradiatively.

Several techniques exist for calculating photonic band structures numerically. The most common method at the moment is the plane wave method (PWM).<sup>25-27</sup> In this method one of the fields, for example  $\mathbf{H}$ , as well as the dielectric constant are expanded in plane waves:

$$\begin{aligned}\mathbf{H}(\mathbf{r}) &= \sum_{\mathbf{G}} \mathbf{H}_{\mathbf{G}} e^{i(\mathbf{k}+\mathbf{G})\cdot\mathbf{r}} \\ \varepsilon^{-1}(\mathbf{r}) &= \sum_{\mathbf{G}} \varepsilon_{\mathbf{G}}^{-1} e^{i\mathbf{G}\cdot\mathbf{r}}\end{aligned}\quad (3)$$

Here, the  $\mathbf{G}$  run over all reciprocal lattice vectors. The expansions are then substituted into the Maxwell equations and a cutoff is made. Increasing the number of plane waves (i.e. the number of  $\mathbf{G}$ 's) will yield an increasingly accurate band structure. Thus, it was shown that there is no complete band gap between the 2<sup>nd</sup> and 3<sup>rd</sup> bands for any fcc lattice of spheres. On the other hand, the diamond lattice, consisting of an fcc lattice with two spheres per unit cell, does have a complete band gap.<sup>27</sup> It occurs for the direct crystal structure at a refractive index contrast above 2.0. Some time later, however, it was shown

that also the fcc structure has a complete gap, but between the 8<sup>th</sup> and 9<sup>th</sup> bands and only for the inverted crystal.<sup>28</sup> This work also pointed out some convergence problems with the PWM and provided an extrapolation method to handle these problems. This has led to improvements in the accuracy of the calculated gap widths. An experimental problem of interest is to insert lattice defects into the crystal. These may lead to donor or acceptor states, or allow wave guiding. Numerical calculation of such defect structures is possible in the plane wave framework using the supercell method.<sup>29,30</sup>

For comparison with experiments a calculation is needed of the transmission or reflection spectrum of a finite-sized photonic crystal. These are not easily obtained with the PWM, which only yields the band structure of an infinite crystal. This problem can be circumvented using the transfer matrix method (TMM).<sup>31,32</sup> The system is then divided into small cells and the fields in each cell are related to those in the previous by a transfer matrix. On the incident side the fields are coupled to a set of plane waves. This method also uses less computer time and memory than the PWM, and can be applied more easily to crystals with defects or crystals in which the dielectric constant is frequency dependent or has an imaginary part.

Another efficient method is the photonic version of the Korringa-Kohn-Rostoker (KKR) method, which was originally developed to describe multiple scattering of electrons in crystals. The scattered field of individual scatterers is expanded in spherical harmonics and the band structure is obtained from a secular equation.<sup>22,33</sup> This method converges much more quickly than the PWM and can easily be used with frequency-dependent or complex dielectric constants. If transmission and reflection spectra of finite crystals are required then the scattering matrices of individual layers of scatterers are determined.<sup>34-36</sup> The method is then referred to as the layer KKR (or LKKR) method.

Finally, especially if the time dependence of the fields inside photonic crystals is of interest finite difference time domain (FDTD) techniques are often used.<sup>37</sup>

Two approximate theories must be also mentioned here, which are often used for comparison with experimental data because they yield simpler, analytical results. These are the dynamical diffraction theory (DDT) of X-ray diffraction,<sup>19,20</sup> which has been quite successful in describing optical diffraction by colloidal crystals.<sup>38-40</sup> The other is now called the scalar wave approximation (SWA), and similarly describes this diffraction well.<sup>41,42</sup> In essence, these two approximate theories are very similar. The starting points are the wave equation for the displacement field  $\mathbf{D}$  in the DDT or the scalar wave equation for the electric field  $E$  in the SWA. In both cases the field in the crystal is expanded in plane waves, as in the PWM, but only the two strongest ones are kept (corresponding to the incident wave and a diffracted wave). Both theories perform reasonably well for wave vectors close to a reciprocal lattice point (where one diffracted wave is much stronger than the others) and become exact in the limit of small refractive index contrast. Experiments suggest that the SWA performs better for larger index contrast,<sup>43</sup> but it has the disadvantage that it cannot describe polarization effects unlike the DDT.<sup>39,40,44</sup> (For completeness it should be remarked that the name scalar wave approximation was originally used for the full plane wave method, but starting from the scalar wave equation.<sup>45,46</sup> These calculations were quickly superseded by the PWM starting from Maxwell's vector wave equation when it became clear that the former predicted the existence of complete band gaps, where in fact there were none due to the polarization of the field.)

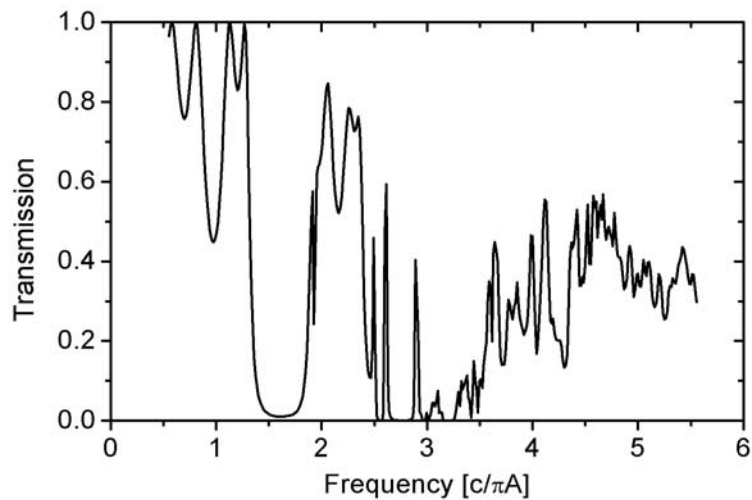


**Figure 3.** Transmission spectrum of a crystal of air spheres in a material with refractive index 3 calculated with the layer KKR method. The crystal is two unit cells thick and the transmission is measured perpendicular to the (111) planes, i.e. the direction of the L point.

## 2.2. Experimental Probes of Photonic Crystals

As mentioned above, an infinitely large, perfect photonic crystal would reflect 100% of the incident light at wavelengths in the band gap and would transmit 100% (apart from a few percent ordinary specular reflection) of the light at other wavelengths. At any given angle of incidence there will be such gaps. In the case of a complete band gap the reflected wavelength bands would overlap at every incident angle. This is the reason that one usually searches for photonic band gaps by measuring transmission or reflection spectra at varying angles of incidence. Ideally, the wavelengths at which the transmission goes from 0 to 1 or from 1 to 0 should correspond to the band edges. This approach was taken in the microwave experiments of Yablonovitch demonstrating that certain crystals made by drilling holes in a dielectric possessed a complete band gap.<sup>12</sup> Similar measurements of the positions and widths of optical stop gaps have become by far the most popular method in the literature.

In practice, however, a number of experimental complications arise. First of all, real photonic crystals are never perfect nor infinite. Due to their finiteness the transmission is rarely close to 0 or 1. In fact, numerical calculations of transmission and reflection spectra often show a lot of structure. This is seen in Figure 3. The extra structure arises when the external wave is coupled to the internal wave using the proper boundary conditions. A considerable part of the wave may be reflected even outside a band gap. Conversely, the transmission inside a band gap does not always drop entirely to zero because, especially near the edges of the gap, the wave may decay with a characteristic length of many unit cells. (Because the wave vector becomes imaginary in the band gap the wave amplitude decays exponentially with distance.) Especially in thin crystals it may therefore not be easy to determine the band edges. This problem is made worse by a

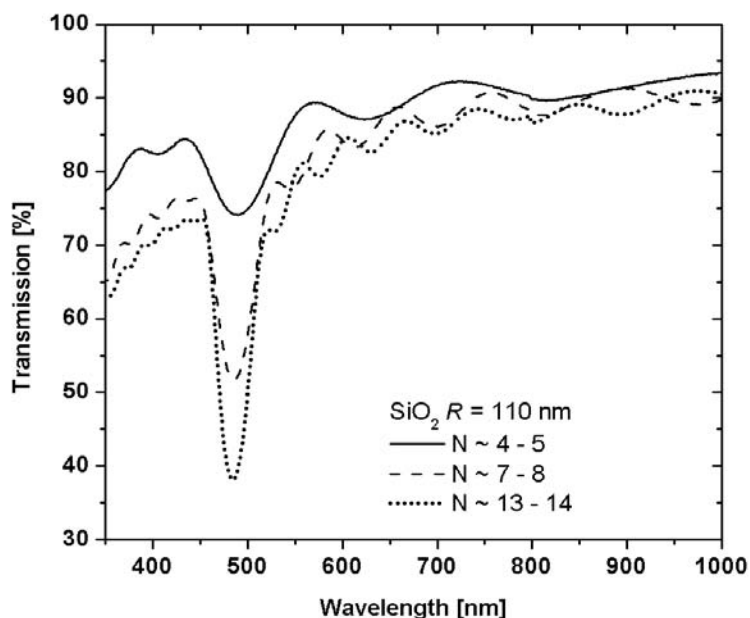


**Figure 4.** Transmission spectra of colloidal crystals of silica spheres (radius 110 nm) with different numbers of layers  $N$ . The crystals were prepared by controlled drying (section 3.4), courtesy of Krassimir Velikov.

certain degree of disorder or the presence of defects, which cause the dip in the transmission to broaden and its edges to become less well defined. Another, but related problem is polycrystallinity of the sample, which often occurs in self-assembled crystals. This will result in a large broadening of the transmitted and reflected bands, because changing the wavelength will successively probe different crystallites having different orientations. In all these cases, simply taking the full width at half maximum is therefore not necessarily the best way to proceed.

These difficulties should be minimized by making sure one is observing a single crystal with as few defects as possible. Polycrystallinity is not normally a problem in crystals made with lithographic techniques, but may be a limitation in self-assembled crystals. It has been shown that gap widths extracted from reflection spectra are much more reliable than those obtained from transmission spectra, because reflected light probes only a small number of lattice planes lying close to the surface<sup>47</sup> (thus containing fewer domains with fewer defects). One should therefore reduce the probe beam to a size smaller than a single crystalline domain. Reducing the beam size even further to much less than the domain size will further reduce the influence of defects and surface roughness. This was beautifully demonstrated in reflection and luminescence spectra measured with the use of an optical microscope.<sup>48</sup> Alternatively, polycrystallinity can be avoided by growing large single crystals, which are not too thick (see section 3.4), so that transmission spectra also produce accurate gap widths.<sup>49,50</sup> An example of a transmission measurement done on such a sample is shown in Figure 4. The transmission minimum becomes deeper and narrower as the number of layers is increased. The ripples are Fabry-

Perot fringes caused by interference of light reflected from the top and bottom surfaces of the crystal. The transmission of the crystals decreases gradually at shorter wavelengths due to diffuse scattering by defects.

In studying the band structure and determining the presence of a complete band gap by transmission/reflection measurements one needs to vary the angle of incident light in order to study all directions in the irreducible part of the Brillouin zone. Due to refraction at the crystal surface the direction of the wave inside the crystal will differ from that outside. Although often used, Snell's law is no longer adequate to convert external angles into internal ones, because the effective refractive index changes significantly close to a band gap. Instead, one should use the fact that the component of the wave vector parallel to the surface,  $k_{\parallel} = (\omega / c) \sin \alpha$ , is conserved.<sup>21</sup> It should be realized that this component is different for frequencies corresponding to the lower and upper band edge. In other words: at nonzero angle of incidence the transmission/reflection spectra probe varying crystal directions as a function of wavelength. Especially at higher order band gaps this complicates the interpretation.<sup>51</sup> A related difficulty is that, due to refraction, not all internal directions can be reached with an external beam. Moreover, some wave vectors are reflected by the crystal not because they are in a band gap but because they do not couple to an internal mode for symmetry reasons.<sup>52,53</sup> It is therefore necessary to prepare samples with different lattice planes exposed. Furthermore, complementary band structure calculations, as well as calculations of transmission or reflection spectra are required to confirm the presence of a band gap. This was recently performed with inverted silicon crystals, providing strong indications for the presence of a complete band gap around 1300 nm.<sup>54</sup>

A related technique to investigate photonic crystals is the use of Kossel lines,<sup>55,56</sup> which can be interpreted in terms of the band structure of colloidal crystals.<sup>17,57,58</sup> The crystal is illuminated with a laser beam resulting in dark rings on a diffusely lit background, both in reflection and transmission. The diffuse background originates from scattering by defects or, alternatively, from scattering by an external diffuser. In the directions of the stop gaps the scattered light is attenuated producing dark rings.

Although I have so far focused on transmission and reflection spectra, an alternative approach makes use of internal sources. These may be fluorescent dyes, luminescent ions, or quantum dots. The effect of the crystal upon their emission is twofold. First, emitted radiation is Bragg diffracted leading to a dip in the measured emission spectrum that depends on the direction of observation, similar to Kossel lines. This effect is present in every photonic crystal and does not require a high dielectric contrast. Second, the spontaneous emission rate can be modified if the photonic crystal alters the local photonic density of states. This effect has been one of the earliest promises of photonic crystals.<sup>10</sup> For an atom with a transition frequency in a complete photonic band gap the spontaneous emission should be inhibited and a quantum electrodynamic photon state bound to the atom is formed.<sup>59,60</sup> A reduction of the LDOS should be measurable as an increase in the radiative lifetime (in a time dependent measurement) or as an overall reduction of the total amount of emitted light (in a stationary state experiment). This effect is often regarded as one of the most important goals in photonic crystal research. Nevertheless, the filtering effect is still very useful as a probe to investigate the band structure of the crystal.<sup>61-69</sup>

It can be safely said that the distinction between the two effects of a photonic crystal on emission has not always been very clear in the literature so far. This has been caused in part by chemical effects of the environment of dye molecules on the radiative lifetime (for example when they are absorbed to particle surfaces). Secondly, the LDOS may already be modified strongly by a microcavity effect due to scattering resonances in microdroplets or colloidal spheres<sup>70-73</sup> or close to surfaces.<sup>74,75</sup> Although this is also a quantum electrodynamic effect it is not due to the photonic crystal. In colloidal crystals of polystyrene spheres suspended in water containing a dye a change in lifetime by a factor of 1.8 was found,<sup>76</sup> but it has been suggested that this could have been caused by chemical interactions and dye adsorption.<sup>71,77,78</sup> A change to nonexponential fluorescence decay has been observed in dye-doped polymer-filled opals.<sup>79</sup> In both these examples the density of states is expected to have changed only a few percent due to the low refractive index contrast.<sup>80</sup> Such a small change was demonstrated experimentally for silica spheres in which the dye had been incorporated deep inside the spheres to avoid chemical interactions with the solvent or particle surfaces.<sup>81,82</sup> A wavelength resolved demonstration of changes in lifetime as the wavelength is scanned through the band gap is still lacking. Instead of a change in lifetime one may also search for an overall reduction in emitted intensity due to a lower density of states and compare it to a suitable reference sample.<sup>83-86</sup> In three-dimensional titania “air-sphere” crystals, in which propagation of light is restricted to 45% of all available directions such inhibition of spontaneous emission was recently seen.<sup>86</sup>

Other optical probes of photonic band gaps rely on the fact that close to a band gap the photon dispersion relation  $\omega$  vs.  $k$  deviates from linearity. This means that the refractive index  $n = ck/\omega$  associated with a band becomes frequency dependent. This index change can be determined by measuring the phase change  $\Delta\phi(\omega)$  of a transmitted laser beam in an interferometer as the frequency is tuned through the gap.<sup>87,88</sup> Close to the lower band edge the index decreases by an amount depending on the gap width, while it increases near the upper band edge. The dispersion relation can be determined from  $k(\omega) = \omega/c + \Delta\phi/L$ , where  $L$  is the sample thickness.

A stronger effect can be seen in the group velocity  $v_g = d\omega/dk$  which vanishes at the edges of the Brillouin zone, where the bands are horizontal. Short laser pulses should thus slow down if their frequency is tuned to the band edges, an effect which was measured in colloidal crystals and artificial opals.<sup>89,90</sup> The effect on the travel time of a pulse is shown in Figure 5. The largest time delay corresponds to a pulse velocity of about 80% of that far from the gap. Such a pulse experiences an increased effective path length due to multiple reflections in the crystal. Because ultrashort laser pulses consist of a finite frequency bandwidth their different frequency components suffer different delays, resulting in a “chirped” pulse. Using ultrashort pulse interferometry the relative phase shift of these frequency components can be measured.<sup>89</sup> This is expressed in a quantity called the group velocity dispersion (GVD)  $\beta_2 = d^2k/d\omega^2$ , also shown in Figure 5. It is further seen that when such a measurement is done in reflection the GVD is near zero inside the gap, but very large just outside. Thus, the GVD naturally locates the edges of the stop gaps without further interpretation being necessary.

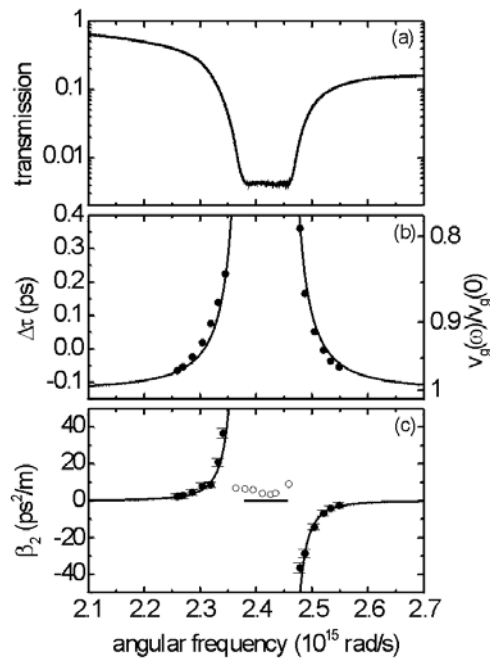


**Figure 5.** (a) Transmission spectrum of a colloidal crystal of polystyrene spheres in water. (b) Measured pulse delay times near the L gap versus angular frequency. The right axis shows the pulse velocity relative to the velocity away from the gap. (c) Measured group velocity dispersion. Solid symbols are transmission, open symbols reflection measurements. The lines in (b) and (c) are the dynamical diffraction theory.

### 3. FABRICATION OF PHOTONIC CRYSTALS

Numerical calculations have led to the identification of a number of three-dimensional crystal structures that should have a complete photonic band gap. Fabrication of these structures on a submicrometer length scale is still a challenge, especially because materials with a sufficiently high refractive index and negligible absorption have to be used. Suitable materials are often semiconductors such as  $\text{TiO}_2$ , Si, or GaAs. The structures must also have a very high porosity, typically containing  $\sim 80\%$  air. A number of strategies has been developed. I will first briefly discuss nanofabrication techniques that use lithography and etching, or holography. Then, I will treat methods that use colloidal self-assembly to fabricate the desired structures, as well as templating methods to obtain inverse colloidal crystals. Then a number of methods will be described that use an external field or a surface template for directing self assembly to produce better ordered or more favorable structures. In the last subsection the effects of disorder and lattice defects will be discussed.

#### 3.1. Nanofabrication

Compared to their success in the fabrication of two-dimensional photonic crystals modern semiconductor processing techniques have so far had relatively limited success in

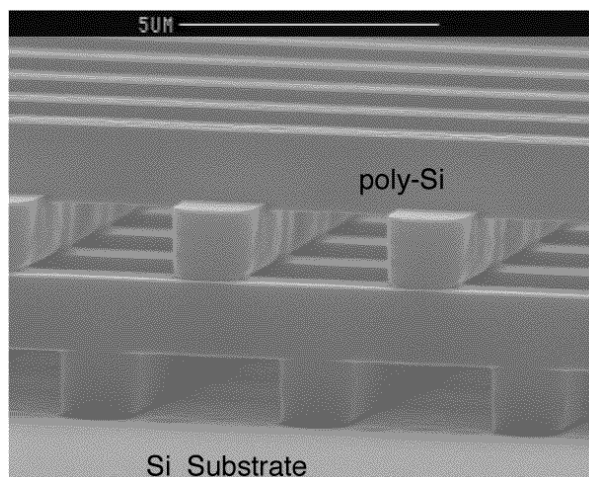


**Figure 6.** Scanning electron micrograph of the silicon woodpile structure. The width of the rods is 1.2  $\mu\text{m}$ . Courtesy of Sandia National Laboratories. Reprinted by permission from Nature,<sup>14</sup> copyright (1998) Macmillan Publishers Ltd.

producing three-dimensional structures. A promising approach is the layer-by-layer preparation of the so-called woodpile structure (Figure 6), which is known to have a complete band gap.<sup>91,92</sup> Each layer consists of a number of parallel silicon rods with a square cross section. These are made by depositing a layer of  $\text{SiO}_2$ , etching out rectangular grooves and filling them with polycrystalline silicon. Then a subsequent layer is deposited and the process is repeated with the grooves rotated  $90^\circ$ . Finally, the  $\text{SiO}_2$  is removed completely. While the original structures exhibited a band gap at a wavelength of about 11  $\mu\text{m}$ ,<sup>14</sup> sizes were later reduced to produce a band gap around 1.5  $\mu\text{m}$ .<sup>15</sup> However, it is a very time-consuming method and has been carried out to only 5 layers, or 1.25 unit cells. Instead of depositing layers one by one it is also possible to fabricate this structure from III-V semiconductors by successively stacking and bonding patterned wafers after careful alignment.<sup>16</sup> This way the number of layers can be increased more quickly and a total of 8 layers has been achieved.

An alternative method is the use of chemically assisted ion beam etching to drill narrow channels into a GaAs or GaAsP wafer<sup>93,94</sup> in a manner similar to that used by Yablonovitch, but on a much smaller length scale. The depth reached was only 1.5  $\mu\text{m}$ , or 4 crystal layers. Using focused-ion-beam etching the same structure with a band gap at 3  $\mu\text{m}$  could be made in silicon up to a depth of 5 unit cells.<sup>95</sup>

Photo-assisted electrochemical etching of pre-patterned silicon has been used to produce a two-dimensional array of very deep ( $\sim 100$   $\mu\text{m}$ ) cylindrical holes.<sup>96</sup> By modulating the light intensity in time it is possible to induce a periodicity of up to 25 periods in the vertical direction.<sup>97</sup> So far, this periodicity is relatively large compared to that in the horizontal directions, so that the structure does not yet possess a complete photonic band gap.

A final method mentioned here uses three-dimensionally periodic patterns of light created by interfering up to four laser beams,<sup>98,99</sup> similar to holographic recording. The

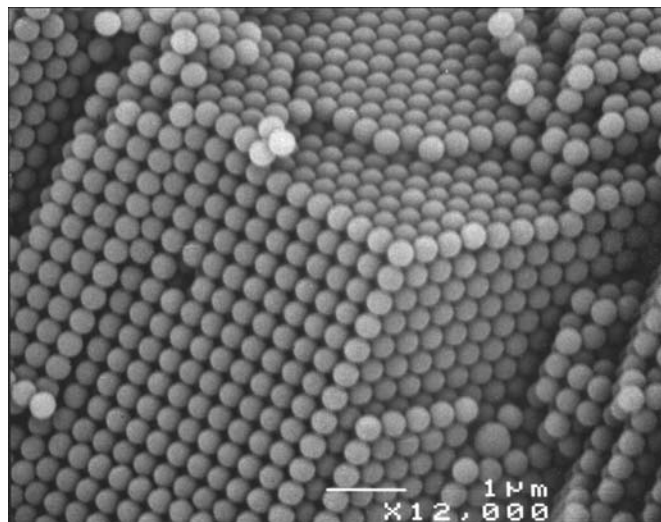


**Figure 7.** Scanning electron micrograph of a polystyrene colloidal crystal. Planes with hexagonal and square symmetry can be seen indicating that the lattice is fcc.

pattern is recorded in a film of photoresist. Unpolymerized resin is then removed by washing. The method is suitable for quickly producing large-area crystals with any desired structure, as long as the polymerized regions are interconnected. Absorption of the light by the photoresin limits the maximum thickness of the crystals to several tens of  $\mu\text{m}$ 's, corresponding to several tens of lattice planes. Since photoresists have a relatively low refractive index additional steps (such as templating, section 3.3) must be used to increase the dielectric contrast.

### 3.2. Self-Assembly Methods

Monodisperse colloidal particles can spontaneously organize into three-dimensionally periodic crystals with a macroscopic size (Figure 7). Their lattice periodicity is easily adjusted from the nanometer to the micrometer range by varying the size of the particles. Colloidal crystals form spontaneously if there is a thermodynamic driving force, for example a sufficiently high particle concentration, making it favorable for the particles to order into a lattice, thus using the limited space more efficiently. When left undisturbed most colloidal particles settle to the bottom of their container where their concentration becomes high enough for crystallization. This process is sometimes accelerated by centrifugation or by filtration of the liquid through a porous membrane. Alternatively, ion exchange resin can be added to the suspensions to increase the range of repulsion between the particles, which leads to crystallization. Typical crystal sizes are from tens to thousands of micrometers. The crystal structure formed in most cases is face centered cubic (fcc), although low volume fraction body centered cubic (bcc) crystals form if the particles interact repulsively over distances much longer than their sizes.<sup>100</sup> Particles which interact nearly as hard spheres show a tendency to form randomly stacked hexagonal layers. In this structure the stacking order of the hexagonally

packed (111) planes is not ABCABC... as in fcc, nor ABAB... as in hcp, but close to random.<sup>101,102</sup>

Their self-organizing properties make spherical colloids suitable candidates for fabricating photonic crystals. There are only a few materials from which colloids can be made with sufficient monodispersity to crystallize, namely silica, ZnS, and a number of polymers, most notably polystyrene and polymethylmethacrylate. Colloidal crystals of most of these materials have a relatively modest refractive index contrast, even when dried. A lot of work has been done on the fabrication and photonic properties of both suspended and dried colloidal crystals, often called artificial opals, and even natural opals.<sup>17,18,61,62,103-108</sup> In this work, the influence of photonic band structures on diffraction was investigated, mostly using angle-dependent transmission and reflection measurements. The influence of the dielectric contrast was established by infiltrating the opals with various liquids or semiconductors (such as CdS or InP), and the sphere filling fraction was varied by gradual sintering of the spheres. The influence of sintering has also been investigated theoretically with the PWM<sup>24</sup> and the TMM.<sup>109</sup> As already discussed in section 2.2 self-assembled crystals have also been filled with luminescent materials in order to study their influence on emission.<sup>61-69</sup>

### 3.3. Colloidal Crystal Templating

Despite this progress the early calculations had already shown that the prevailing fcc structure possesses a complete photonic band gap only for the inverted crystal structure, in which the spheres have a lower index than their environment.<sup>28</sup> Furthermore, the refractive index contrast needs to be very large ( $>2.85$ ). Although the diamond structure has a complete band gap for the direct crystal structure<sup>27</sup> it is never formed in colloidal self-assembly. More detailed calculations of the photonic properties of crystals formed by self-assembling systems determined that the optimal air filling fraction was around 80%,<sup>24,110,111</sup> but did not identify structures that are easier to fabricate. These facts quickly led to the development of chemical means by which the interstitial pores of a colloidal crystal can be filled with a high index solid, after which the colloidal particles can be removed.<sup>112-118</sup> These approaches are known collectively as templating methods. In that way, the air filling fraction of such an “inverse opal” is automatically close to the maximum sphere packing fraction of 74% and a larger variety of materials can be used. A general schematic of colloidal crystal templating is shown in Figure 8. First, a colloidal crystal is assembled from a monodisperse colloid. Then the fluid in the interstitial pores is either gelled directly through a sol-gel process or by a polymerization reaction, or it is removed first by drying and then replaced by infiltration of the pores with a solid or a solidifying liquid. In the third step the colloidal template is removed from its solidified environment by dissolution, evaporation, or firing at temperatures of up to 400 °C. This final step often also involves calcination of the material at elevated temperatures in order for the resulting porous framework to densify and crystallize. The uncalcined material is often amorphous and contains micro- and mesopores that lower its refractive index. Calcination frequently results in shrinkage of the porous material by up to 20%. Examples of some resulting materials are shown in Figure 9.

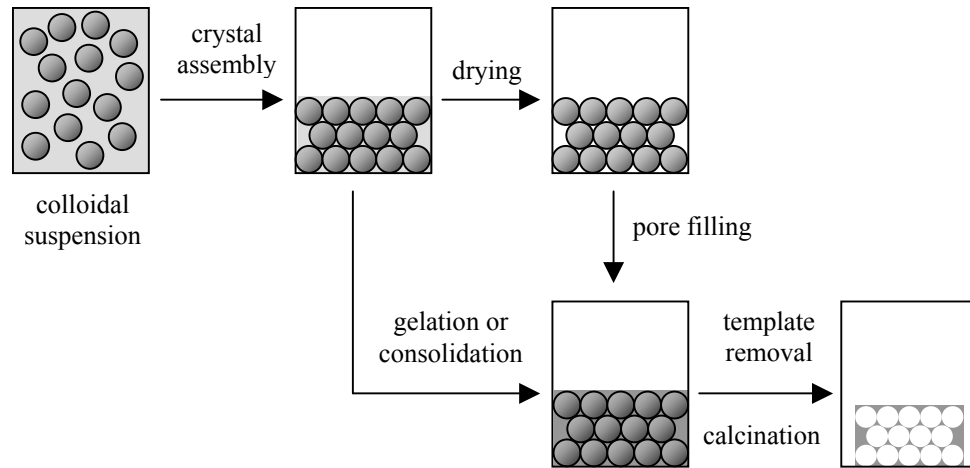
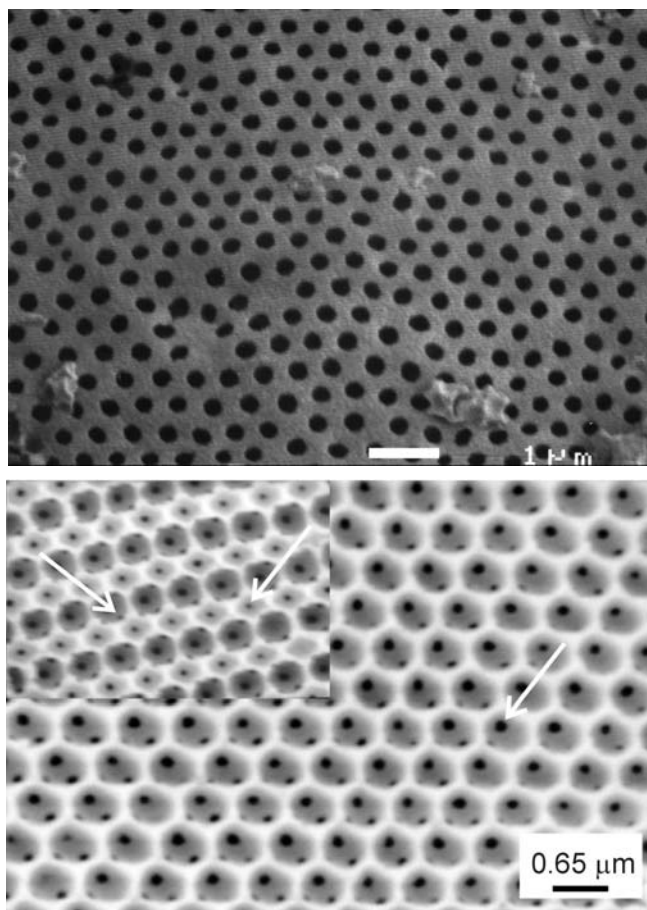


Figure 8. Schematic of colloidal crystal templating.

They form a faithful replica of the original colloidal crystal, including lattice defects such as vacancies. The spherical voids left behind by the spheres are usually connected by windows where the spheres touched, allowing material to be transported during template removal.

The initial templating methods used emulsion droplets<sup>112</sup> or polystyrene spheres<sup>114,116,118</sup> as the colloidal template, and sol-gel chemistry to fill the interstitial space. Using emulsion droplets ordered porous materials of titania ( $\text{TiO}_2$ ), zirconia ( $\text{ZrO}_2$ ), silica, and polyacrylamide were made.<sup>112,113</sup> The emulsion oil droplets are not easy to make monodisperse, but they are easy to remove by dissolution or evaporation. A calcination step then converted the titania gel into the desirable high refractive index titania phases anatase ( $n=2.5$ , above  $400^\circ\text{C}$ ) or rutile ( $n=2.8$ , above  $900^\circ\text{C}$ ).<sup>120</sup> In independent work polystyrene latex spheres and a sol-gel reaction were used to produce inverted crystals of amorphous silica.<sup>114,115</sup> Because polystyrene spheres are easy to obtain with high monodispersity and because they self-assemble with great ease they have been used in many subsequent templating studies.<sup>116,117,121-124</sup> These particles are removed either by calcination or by dissolution in, for example, toluene. Monodisperse polymethylmethacrylate spheres may be used similarly.<sup>125</sup> Silica spheres can be made equally monodisperse as polymer colloids, but must be removed by etching with a hydrogen fluoride (HF) solution.<sup>54,126-130</sup> All these approaches have resulted in materials containing large domains of well-ordered spherical pores.

The type of material that is desired often limits the methods available for pore filling. For photonic crystals the desired material is obviously one with a high refractive index and a low absorption. For this purpose titania and silicon have so far been the most successful; broad stop gaps have been measured in inverted opals made of these materials.<sup>47,54,123,130</sup> But inverted opals have also been made for many other applications, such as catalyst supports, filtration and separation materials, and thermal insulators. This explains the large variety of different materials that have been used in colloidal crystal templating. This work will now be reviewed briefly. In all cases, it is important that the



**Figure 9.** (Top) Titania inverse crystal prepared by emulsion templating. (Bottom) Titania inverse crystal made by templating polystyrene spheres, with (111) and (110) faces (inset) exposed, courtesy of Willem Vos.

interstitial space of the crystal be sufficiently filled and contiguous, or else the structure will collapse during template removal.

Many metal oxides (titania, silica, zirconia, alumina, yttria, etc.) are produced by hydrolysis of the corresponding liquid metal alkoxide, which is infused into the pores by capillary action, sometimes aided by suction.<sup>116-118,122-124</sup> The alkoxides may be diluted in alcohol to lower their viscosity. After hydrolysis, the process is repeated several more times to increase the degree of filling. In some cases small openings in the center of the interstitial sites are left open when the channels connecting them have become blocked.<sup>118</sup> Calcination of materials prepared in this way sometimes leads to excessive grain growth so that the periodic pore structure may be lost. For this reason, rutile titania could not be prepared this way, unlike the case with emulsion templating.<sup>112</sup> An alternative approach is to use ultrafine powders of silica or nanocrystalline rutile, which are added to a monodisperse polystyrene latex. The mixed suspension is then dried slowly to produce an ordered macroporous material in one step.<sup>131-134</sup> Similar approaches using 4 nm CdSe

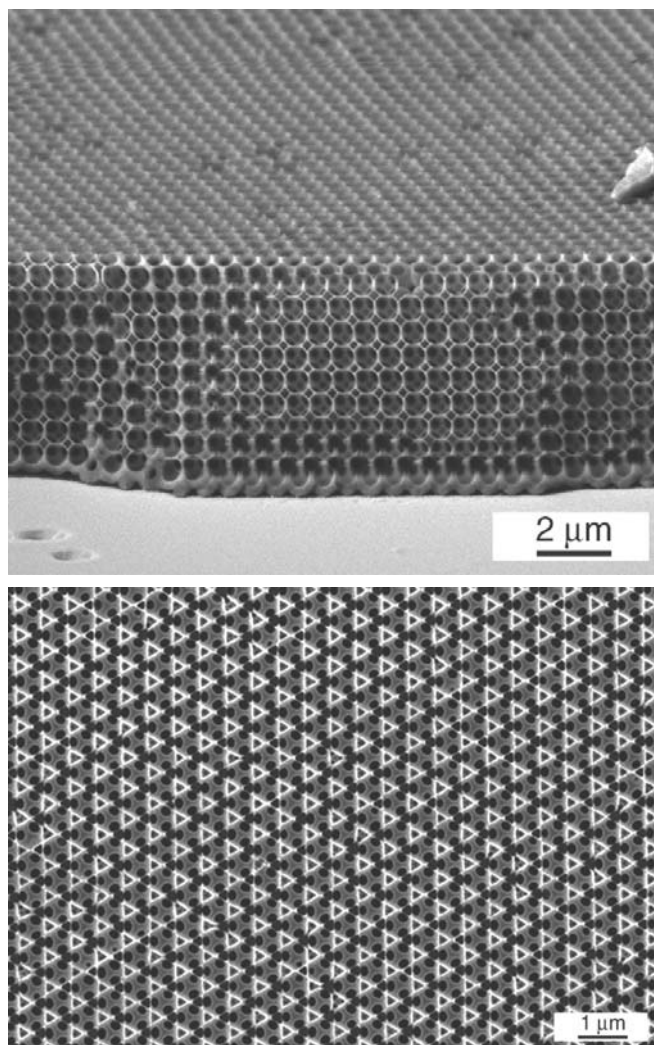


**Figure 10.** Porous silicon by templating of silica spheres using CVD. Top picture shows a sample edge with a (100) surface. Bottom picture is a (111) surface exposed by reactive ion etching. Courtesy of David Norris, reprinted by permission from Nature,<sup>54</sup> copyright (2001) Macmillan Publishers Ltd.

quantum dots<sup>128</sup> and gold nanocrystals<sup>135,136</sup> have also been used. Due to the small size of the particles efficient pore filling is achieved.

Polymeric inverted opals have been made of polyacrylamide, polystyrene, polymethylmethacrylate, and polyurethane by infiltrating colloidal crystals with a liquid monomer followed by heating or exposure to UV light to initiate the polymerization.<sup>83,113,126,129,137-139</sup>

Precipitation reactions of salts followed by chemical conversion have been applied to expand the variety of accessible materials to a large number of carbonates and oxides of

metals which cannot be prepared by sol-gel chemistry.<sup>140</sup> Subsequent reduction with hydrogen gas has produced ordered macroporous Ni.<sup>141</sup> Similarly, reduction of sol-gel derived germanium oxide has been used to make macroporous germanium, which is transparent in the infrared ( $\lambda > 1900\text{nm}$ ) where the refractive index is as high as 4.

Electrochemical deposition can also be used to template colloidal crystals that have been deposited on an electrode. This way ordered macroporous CdS, CdSe<sup>142,143</sup> and Au<sup>144,145</sup> have been prepared. A variety of porous metals has been made by electroless deposition in silica crystals functionalized with gold nanocrystals.<sup>146</sup> Alternatively, opals can be infiltrated with molten metals at increased pressure.<sup>147</sup>

A final templating method is chemical vapor deposition (CVD), with which the degree of filling can be accurately controlled. Thus, CVD was used to fill silica crystals with graphite and diamond,<sup>127</sup> silicon, which has a refractive index of 3.5 and is transparent at wavelengths above 1100 nm,<sup>130</sup> and germanium.<sup>148</sup> A difficulty was the obstruction with material of the outermost channels which provide access to the innermost channels. Using low-pressure CVD, which prevented channel obstruction, and highly ordered silica crystals, inverted crystals of silicon were made.<sup>54</sup> The resulting material is shown in Figure 10. By measuring two different crystal orientations and comparing reflection and transmission spectra with numerical calculations the authors were able to show that their crystals probably possess a complete photonic band gap around 1300 nm.

### 3.4. Directed Self-Assembly: More Order and Different Lattices

Although colloidal self-assembly has distinct advantages in the fabrication of three-dimensional photonic crystals it also has a number of drawbacks. Without gentle persuasion the material formed is polycrystalline, contains lattice defects and stacking errors, and can only form a limited number of crystal structures, which have a random orientation. A number of strategies have been developed to overcome these limitations. Methods in which an external influence is used to direct particles to preferred lattice positions will be called directed self-assembly techniques.

A relatively simple technique that already produces well-ordered crystals is called convective self-assembly or controlled drying. It was originally developed for the fabrication of two-dimensional crystals from colloidal spheres,<sup>149,150</sup> but has been extended to allow the formation of three-dimensional crystal films of up to 50 layers in one step.<sup>151</sup> The process is shown schematically in Figure 11. A clean and flat substrate such as microscope slide is placed vertically in a colloidal suspension. As the solvent evaporates from the meniscus more particles are transported to the growing film by fluid flow. Capillary forces in the drying film pull the spheres into a regular close packing. The number of layers can be controlled accurately by the particle volume fraction. The resulting crystal has a uniform orientation over centimeter distances, making it essentially single-domain. Although vacancies exist their number is relatively small. Cracks often form during drying but the crystal orientation is preserved across cracks. Sedimentation of particles larger than about 0.5  $\mu\text{m}$  prevents their deposition in this way. However, this problem can be overcome by applying a temperature gradient which causes a convective flow counteracting sedimentation.<sup>54</sup> Controlled drying has produced some of the best

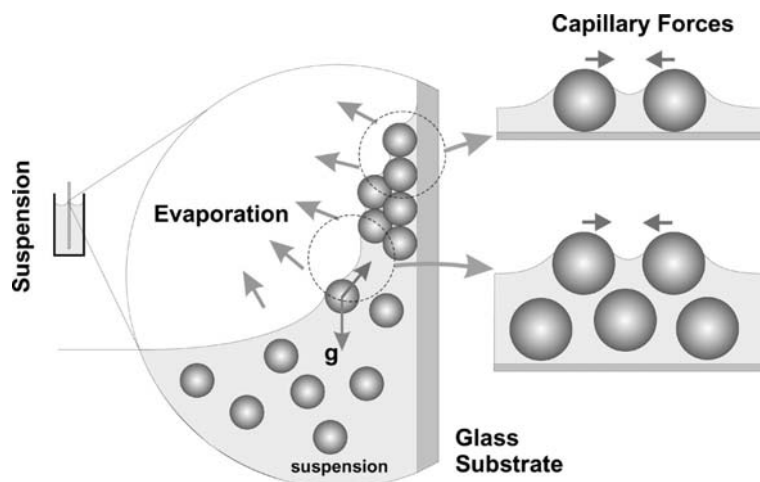


**Figure 11.** Schematic of controlled drying. See text for explanation.

ordered colloidal crystals, which are suitable for investigating the optical properties of photonic crystals (see Figure 4), both the direct and inverted structures.<sup>49,50,54,151,152</sup>

Another approach to assembly of well-ordered, large-area crystals of close-packed spheres is to filter colloidal spheres into a thin slit between two parallel plates.<sup>153-155</sup> The crystal thickness can be controlled from a monolayer to several hundreds of layers through the plate separation. Fabrication of the filter cells uses photolithography and cleanroom facilities, but an easier method has been developed using replica molding against an elastomeric mold.<sup>156</sup>

Long-range fcc order has also been induced by applying shear flow to a concentrated colloidal suspension enclosed between parallel plates.<sup>157</sup>

Although electrophoretic deposition is widely used for the deposition of particulate films of many different materials it can also be used to prepare ordered three-dimensional sphere packings.<sup>158-161</sup> The quality of the crystals formed appears to be comparable to that obtained by sedimentation, but is somewhat lower than that in crystals formed by controlled drying. It is much faster, however.

The methods to direct colloidal self-assembly mentioned thus far produce (nearly) close packed crystals of the fcc type. Their (111) planes are always arranged parallel to the substrate. Other directed self-assembly methods try to overcome these limitations.

In colloidal epitaxy the colloidal particles sediment onto a substrate that has been patterned lithographically with a regular pattern of pits roughly half a particle deep.<sup>162,163</sup> The first particles fall into the pits, providing a template for other particles. When the first layer was forced to be a (100) or (110) lattice plane of fcc this orientation of the growing crystal was preserved over thousands of layers with relatively few defects. Crystals prepared in this way have recently been templated with selenium.<sup>164</sup> By providing a surface template with a pattern that is unique to the hcp structure a hexagonal close packed crystal grew for tens of layers.<sup>165</sup> Defect lines in the template are reproduced in the successive layers, opening the possibility to construct waveguide structures.<sup>162</sup>

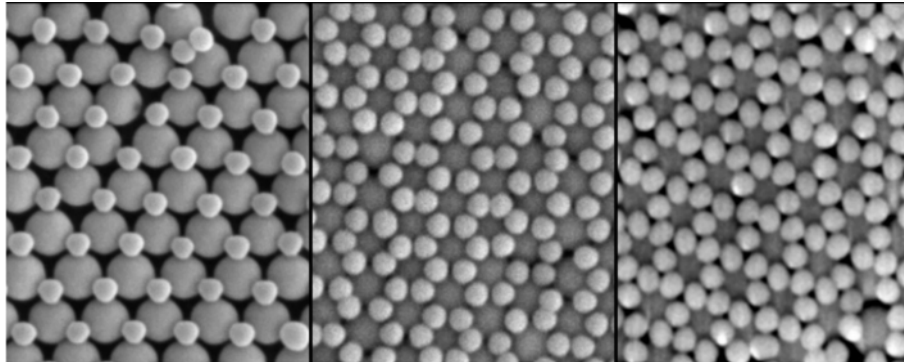


**Figure 12.** Binary crystal structures AB, AB<sub>2</sub>, and AB<sub>3</sub> fabricated using controlled drying, courtesy of Krassimir Velikov.

Another possibility of this method is to make surface templates with a lattice mismatch, which could produce non-close-packed crystals. In an extension of this work (100)-oriented fcc crystals have also been made by patterning the surface with much larger pyramidal pits.<sup>166</sup>

Colloidal crystals can also form binary crystals if the size ratio between the two types of spheres is carefully adjusted. The binary structures AB, AB<sub>2</sub>, AB<sub>4</sub>, and AB<sub>13</sub> have been observed.<sup>167,168</sup> Binary crystal structures also occur in natural opals.<sup>6</sup> At present, no band structure calculations of such lattices have been reported. Binary crystal AB, AB<sub>2</sub>, and AB<sub>3</sub> can be made layer-by-layer by controlled drying.<sup>169</sup> This is shown in Figure 12. If the two types of particle are made of different material then new crystal structures can be made by selectively removing one of the two types. This was demonstrated for a crystal of silica and polystyrene spheres from which the latter were removed by calcination,<sup>169</sup> leading to a stack of hexagonal planes in an AAA... sequence.

Different crystal structures can also be made by making the interaction potential between the colloidal spheres anisotropic. For example, dipolar interactions can be induced by applying a high-frequency electric field. This results in self-assembly of a body-centered tetragonal crystal structure.<sup>170</sup>

Using optical tweezers or other more advanced techniques of single-particle manipulation it should be possible to build many more crystal structures. Although these techniques are better called ‘direct assembly’ rather than directed self-assembly we mention them because they may lead to the fabrication of any desired crystal structure. The most interesting structure is the diamond lattice because it has a complete band gap at an index contrast larger than 2.0. Since the gap appears in the first order Bragg region it would also be less vulnerable to lattice disorder. A recent paper proposed building a diamond lattice from two types of spheres, one of which should eventually be removed,<sup>171</sup> using a technique called robot-aided micromanipulation.<sup>172</sup>

### 3.5. The Effects of Disorder

A certain amount of disorder will be present in all real photonic crystals. Although especially relevant for materials formed by self-assembly disorder also occurs in those

made by nanofabrication. Nevertheless, the effects of disorder on light propagation in photonic crystals has received only modest attention, although John already discussed disorder in periodic lattices in terms of Anderson localization.<sup>11</sup> Effects on transmission and reflection spectra were already briefly mentioned in section 2.2. The length scale that characterizes the degree of disorder as seen by the light used to probe the material is the transport mean free path  $l$ . This quantity is the distance over which light propagates before its direction is randomized by random scattering. If the sample thickness  $L$  is greater than  $l$  the transmission gaps will be broadened by disorder. Broadening was seen in colloidal crystals in which a small number of spheres with different size was deliberately added, as well as impurity modes in the stop gap.<sup>88,173</sup> In reflection measurements only a small depth is probed, determined by the attenuation length of the light, but this depth depends strongly on the wavelength close to the gap. The transport mean free path can be obtained by measuring the total transmission (sum over all angles) as a function of  $L$ , or from enhanced backscattering. There exist only a few reports in which photonic crystals have been characterized this way.<sup>174-177</sup> In all cases the crystals had been made by self-assembly without the use of any of the directed self-assembly methods of section 3.4. The value of  $l$  found was in the range of 10-20  $\mu\text{m}$ .

On the theoretical side it has been shown that disorder narrows the width of the band gap in fcc inverse opals, making it disappear already at a modest amount of disorder.<sup>178,179</sup> Disorder was modeled as a variation in sphere sizes and positions. The relatively large effect was attributed to the fact that the gap occurs between high-frequency bands: Photonic crystals with their gap in the first-order Bragg region, as made by lithographic methods,<sup>180,181</sup> or for a diamond lattice of spheres,<sup>182</sup> have been found to be much more robust to disorder. For self-assembled crystals one should therefore aim for an extra wide band gap to leave sufficient margin. The effect of stacking faults, which occur in some self-assembled systems forming randomly-stacked hexagonal lattices, has also been considered. It was found that gaps will in general appear wider in these systems<sup>183</sup> and that higher order gaps should become very difficult to observe.<sup>111</sup>

#### 4. ENGINEERING OF COLLOIDAL PARTICLES: CORE-SHELL, METALLO-DIELECTRIC, AND ANISOTROPIC COLLOIDS

A great advantage of colloidal self-assembly over other methods of fabricating photonic crystals is that the single particle properties can be engineered. The possibilities of such approaches have only just begun to be explored. The most common way is to use composite particles with a core-shell structure, where core and shell consist of different materials. Other approaches use anisotropic particles.

Core-shell colloids are prepared chemically by the successive deposition of layers of different materials around a starting particle (called the 'seed'). A very wide variety of core-shell colloids has been prepared for many different applications.<sup>184</sup> A special type of core-shell particle is the hollow shell particle, made by removing the core by dissolution or calcination. An important advantage of the core-shell approach is that one could make the core consist of a quantum-size nanocrystal, or a shell to contain a fluorescent dye.<sup>185</sup> In this way, the active material could be accurately positioned inside the unit cell, where the local density of states may have a lower or higher value than the total density of

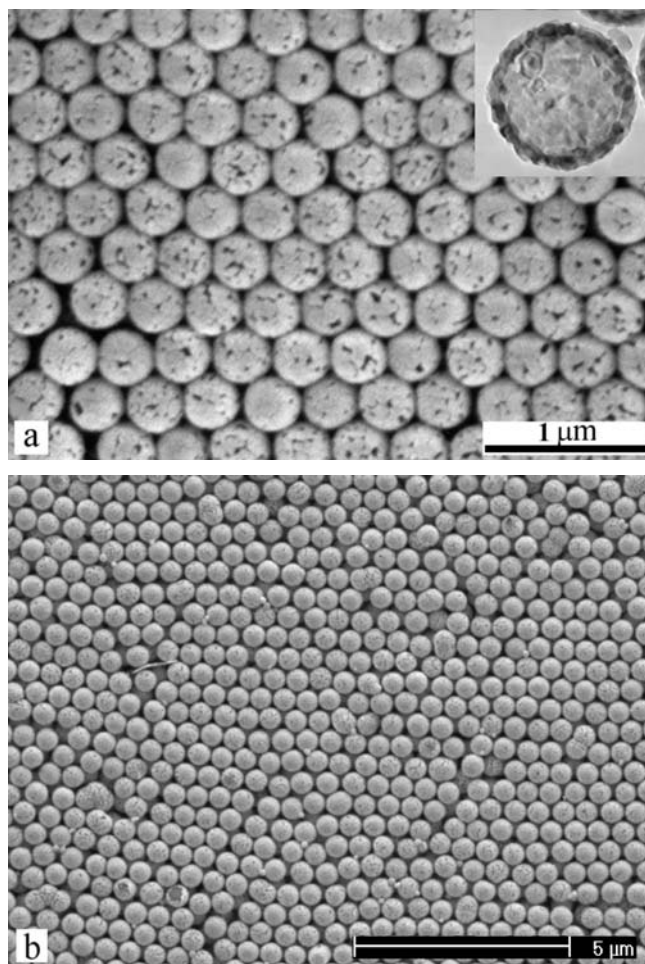


**Figure 13.** (a) Crystal of hollow titania (anatase) spheres. (b) Metallo-dielectric particles consisting of a silica core coated with 32 nm of gold and 10 nm of silica, courtesy of Christina Graf.

states. Another advantage is that defects could be introduced more effectively into a crystal by, for example, substituting some core-shell particles with normal particles of the same size, or vice versa.

Only recently have core-shell colloids been developed for the purpose of making photonic crystals. Crystals made of these colloids are often aimed at producing a wider, and if possible complete, band gap. Thus, fcc crystals of ZnS spheres coated with silica were shown to have a wider L-stopgap than spheres made of pure ZnS or pure silica.<sup>50</sup> The maximum width was reached when the ratio of the core radius to the total radius was about 0.65. Polystyrene spheres coated with a layer of polymer containing CdTe nanocrystals have also been self-assembled into crystals.<sup>186</sup> An apparent widening of the bandgap was, at least in part, due to absorption by the nanocrystals. Hollow shell

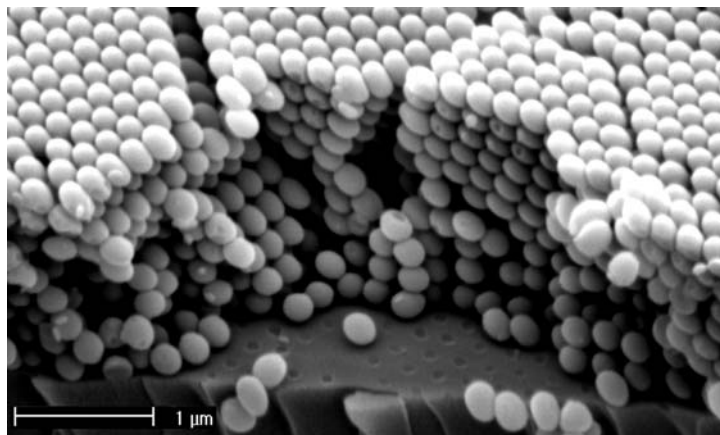


**Figure 14.** A colloidal crystal of ellipsoidal particles made ion irradiation of silica spheres, courtesy of Krassimir Velikov.

particles offer a much higher refractive index contrast and titania has been the favorite shell material.<sup>187-189</sup> An example is shown in Figure 13a. The resulting material is similar to that obtained by colloidal crystal templating, but the spherical voids are now not connected. The core-shell ratio can be varied at will, which is not the case in the templating method.

A complete band gap is not expected for the materials just mentioned, because the refractive index contrast is still too low.<sup>190</sup> This may no longer be the case, however, if metallic or metallo-dielectric particles are used. Theoretical calculations show that fcc crystals of metal spheres, or metal spheres with a dielectric coating, have wide photonic band gaps, originating from the large, negative value of the real part of the dielectric constant.<sup>191-194</sup> However, absorption, due to the imaginary part of the dielectric constant of the metal, could destroy the band gap. Calculations of the transmission, reflection, and absorption spectra of such crystals show that for the noble metals the absorption will be small enough to make such photonic crystals useful at frequencies in the visible and near infrared, with silver performing the best.<sup>194</sup>

A practical consideration is that metal colloids in the required size range can, at present, not be made sufficiently monodisperse. Luckily, the penetration depth of electromagnetic fields into a metal, or skin depth, is on the order of 10 nm at visible wavelengths. One therefore only needs particles with a metal coating that is several tens of nanometers thick. Gold-coated silica spheres have recently been synthesized by depositing gold nanoparticles onto silica spheres.<sup>195,196</sup> A similar approach has been taken for coating silver onto silica<sup>197</sup> or latex<sup>198</sup> spheres. The optical properties of the individual metal shells have been studied,<sup>199-201</sup> showing that they should be useful in optical filters and Raman enhancers. Photonic properties of the crystal have not yet been studied, however. Crystals of gold shell particles were made only recently by coating the metal shells with an extra layer of silica.<sup>196</sup> A dried crystal of these particles is shown in Figure 13b. A further advantage of such silica-gold-silica colloids is that the metal can be accurately positioned at a desired radial position.

As mentioned before, the fcc lattice of dielectric spheres does not have a complete photonic band gap. This can be attributed to a symmetry-induced degeneracy at the W-point of the Brillouin zone. This degeneracy could be lifted by using particles that are anisotropic in shape<sup>202</sup> or in their dielectric properties.<sup>203</sup> This way a complete band gap can open up between the 2<sup>nd</sup> and 3<sup>rd</sup> bands if the anisotropy has the proper size and orientation. There have not been many attempts to construct a colloidal crystal of anisotropic particles experimentally. This is, of course, because there are only a few methods to synthesize these particles with a sufficiently uniform size and shape.<sup>204</sup> Such particles then have to be assembled into three-dimensional colloidal crystals with control over the orientation. This has not yet been achieved, although a few strategies have been suggested by means of external fields and surface templates.<sup>205</sup> An alternative approach is to deform the spheres only after crystal assembly. This has been demonstrated for silica and ZnS spheres by irradiation with high-energy Xe<sup>4+</sup> ions, which deforms the spheres into ellipsoids<sup>206,207</sup> (see Figure 14). The orientation of the ellipsoids can be conveniently controlled through the direction of the bombarding ions. A complication is that not only the spheres are deformed but the fcc lattice as well.

## 5. CONCLUSIONS

In this chapter the fabrication and optical properties of three-dimensional photonic crystals made from colloids has been described. Recent progress has led to the preparation of photonic crystals with a high degree of order and a low defect density. Combination with templating methods has made it possible to achieve the high refractive index contrasts needed for useful photonic applications. The use of core-shell type composite particles or anisotropic particles to tune and improve photonic properties holds great promise for future research. In order to build actual photonic devices with colloidal crystals it will be necessary to insert lattice defects with a high degree of control. This is a much more challenging task in crystals formed by self-assembly than in those made by lithographic techniques. One way of reaching this goal was recently demonstrated by writing waveguide structures into a self-assembled crystal using multi-photon polymerization in a confocal microscope.<sup>208</sup> External control is another important requirement. Indeed, switching of photonic crystals with electric fields has been achieved by filling colloidal crystals with liquid crystals.<sup>209</sup> These examples show that self-assembly of colloidal particles is a powerful way of fabricating three-dimensional photonic crystals.

## 6. ACKNOWLEDGMENTS

The author is grateful to Alexander Moroz for performing the numerical calculations the results of which are presented in Figures 1-3. He, Krassimir Velikov and Alfons van Blaaderen are thanked for useful discussions.

## 7. REFERENCES

1. S. Hachisu, Y. Kobayashi, and A. Kose, Phase separation in monodisperse lattices, *J. Colloid Interface Sci.* **42**, 342-348 (1973).
2. S. Hachisu and Y. Kobayashi, Kirkwood-Alder transition in monodisperse latexes. II. Aqueous latexes of high electrolyte concentration, *J. Colloid Interface Sci.* **46**, 470-476 (1974).
3. P. N. Pusey and W. van Megen, Phase behaviour of concentrated suspensions of nearly hard colloidal spheres, *Nature* **320**, 340-342 (1986).
4. J. V. Sanders, Colour of precious opal, *Nature* **204**, 1151-1153 (1964).
5. J. B. Jones, J. V. Sanders, and E. R. Segnit, Structure of opal, *Nature* **204**, 990-991 (1964).
6. J. V. Sanders and M. J. Murray, Ordered arrangements of spheres of two different sizes in opal, *Nature* **275**, 201-202 (1978).
7. P. L. Flaugh, S. E. O'Donnell, and S. A. Asher, Development of a new optical wavelength rejection filter: demonstration of its utility in Raman spectroscopy, *Appl. Spectrosc.* **38**, 847-850 (1984).
8. G. S. Pan, R. Kesavamoorthy, and S. A. Asher, Optically nonlinear Bragg diffracting nanosecond optical switches, *Phys. Rev. Lett.* **78**, 3860-3863 (1997).
9. J. H. Holtz and S. A. Asher, Polymerized colloidal crystal hydrogel films as intelligent chemical sensing materials, *Nature* **389**, 829-832 (1997).
10. E. Yablonovitch, Inhibited spontaneous emission in solid-state physics and electronics, *Phys. Rev. Lett.* **58**, 2059-2062 (1987).
11. S. John, Strong localization of photons in certain disordered dielectric superlattices, *Phys. Rev. Lett.* **58**, 2486-2489 (1987).
12. E. Yablonovitch, T. J. Gmitter, and K. M. Leung, Photonic band-structure - the face-centered-cubic phase employing nonspherical atoms, *Phys. Rev. Lett.* **67**, 2295-2298 (1991).
13. C. M. Soukoulis (Ed.), *Photonic Crystals and Light Localization in the 21st Century* (Kluwer Academic, Dordrecht, The Netherlands, 2001).
14. S. Y. Lin, J. G. Fleming, D. L. Hetherington, B. K. Smith, R. Biswas, K. M. Ho, M. M. Sigalas, W. Zubrzycki, S. R. Kurtz, and J. Bur, A three-dimensional photonic crystal operating at infrared wavelengths, *Nature* **394**, 251-253 (1998).
15. J. G. Fleming and S. Y. Lin, Three-dimensional photonic crystal with a stop band from 1.35 to 1.95  $\mu\text{m}$ , *Opt. Lett.* **24**, 49-51 (1999).
16. S. Noda, K. Tomoda, N. Yamamoto, and A. Chutinan, Full three-dimensional photonic bandgap crystals at near-infrared wavelengths, *Science* **289**, 604-606 (2000).
17. I. I. Tarhan and G. H. Watson, Photonic band structure of fcc colloidal crystals, *Phys. Rev. Lett.* **76**, 315-318 (1996).
18. W. L. Vos, R. Sprik, A. van Blaaderen, A. Imhof, A. Lagendijk, and G. H. Wegdam, Strong effects of photonic band structures on the diffraction of colloidal crystals, *Phys. Rev. B* **53**, 16231-16235 (1996).
19. W. H. Zachariasen, *Theory of X-Ray Diffraction in Crystals* (Wiley, New York, 1945).
20. R. W. James, *The Optical Principles of the Diffraction of X-Rays* (G. Bell & Sons, London, 1948).
21. M. Born and E. Wolf, *Principles of Optics* (Cambridge University Press, Cambridge, 1999).
22. A. Moroz and C. Sommers, Photonic band gaps of three-dimensional face-centred cubic lattices, *J. Phys. Cond. Matter* **11**, 997-1008 (1999).
23. R. Sprik, B. A. VanTiggelen, and A. Lagendijk, Optical emission in periodic dielectrics, *Europhys. Lett.* **35**, 265-270 (1996).
24. K. Busch and S. John, Photonic band gap formation in certain self-organizing systems, *Phys. Rev. E* **58**, 3896-3908 (1998).
25. K. M. Leung and Y. F. Liu, Full vector wave calculation of photonic band structures in face-centered-cubic dielectric media, *Phys. Rev. Lett.* **65**, 2646-2649 (1990).
26. Z. Zhang and S. Satpathy, Electromagnetic wave propagation in periodic structures - Bloch wave solution of Maxwell equations, *Phys. Rev. Lett.* **65**, 2650-2653 (1990).
27. K. M. Ho, C. T. Chan, and C. M. Soukoulis, Existence of a photonic gap in periodic dielectric structures, *Phys. Rev. Lett.* **65**, 3152-3155 (1990).
28. H. S. Sozuer, J. W. Haus, and R. Inguva, Photonic bands - Convergence problems with the plane-wave method, *Phys. Rev. B* **45**, 13962-13972 (1992).
29. E. Yablonovitch, T. J. Gmitter, R. D. Meade, A. M. Rappe, K. D. Brommer, and J. D. Joannopoulos, Donor and acceptor modes in photonic band-structure, *Phys. Rev. Lett.* **67**, 3380-3383 (1991).
30. R. D. Meade, K. D. Brommer, A. M. Rappe, and J. D. Joannopoulos, Photonic bound-states in periodic dielectric materials, *Phys. Rev. B* **44**, 13772-13774 (1991).

31. J. B. Pendry and A. Mackinnon, Calculation of photon dispersion-relations, *Phys. Rev. Lett.* **69**, 2772-2775 (1992).
32. J. B. Pendry, Calculating photonic band structure, *J. Phys. Cond. Matt.* **8**, 1085-1108 (1996).
33. A. Moroz, Density-of-states calculations and multiple-scattering theory for photons, *Phys. Rev. B* **51**, 2068-2081 (1995).
34. N. Stefanou, V. Karathanos, and A. Modinos, Scattering of electromagnetic-waves by periodic structures, *J. Phys. Cond. Matt.* **4**, 7389-7400 (1992).
35. V. Yannopapas, N. Stefanou, and A. Modinos, Theoretical analysis of the photonic band structure of face-centred cubic colloidal crystals, *J. Phys. Cond. Matt.* **9**, 10261-10270 (1997).
36. N. Stefanou, V. Yannopapas, and A. Modinos, MULTEM 2: A new version of the program for transmission and band-structure calculations of photonic crystals, *Comput. Phys. Commun.* **132**, 189-196 (2000).
37. A. Taflove, *Computational Electrodynamics. The Finite-Difference Time-Domain Method* (Artech House, Boston, 1995).
38. P. A. Rundquist, P. Photinos, S. Jagannathan, and S. A. Asher, Dynamical Bragg-diffraction from crystalline colloidal arrays, *J. Chem. Phys.* **91**, 4932-4941 (1989).
39. Y. Monovoukas, G. G. Fuller, and A. P. Gast, Optical anisotropy in colloidal crystals, *J. Chem. Phys.* **93**, 8294-8299 (1990).
40. Y. Monovoukas and A. P. Gast, A study of colloidal crystal morphology and orientation via polarizing microscopy, *Langmuir* **7**, 460-468 (1991).
41. K. W. K. Shung and Y. C. Tsai, Surface effects and band measurements in photonic crystals, *Phys. Rev. B* **48**, 11265-11269 (1993).
42. I. I. Tarhan and G. H. Watson, Analytical expression for the optimized stop bands of fcc photonic crystals in the scalar-wave approximation, *Phys. Rev. B* **54**, 7593-7597 (1996).
43. D. M. Mittleman, J. F. Bertone, P. Jiang, K. S. Hwang, and V. L. Colvin, Optical properties of planar colloidal crystals: Dynamical diffraction and the scalar wave approximation, *J. Chem. Phys.* **111**, 345-354 (1999).
44. G. S. Pan, A. K. Sood, and S. A. Asher, Polarization dependence of crystalline colloidal array diffraction, *J. Appl. Phys.* **84**, 83-86 (1998).
45. S. Satpathy, Z. Zhang, and M. R. Salehpour, Theory of photon bands in 3-dimensional periodic dielectric structures, *Phys. Rev. Lett.* **64**, 1239-1242 (1990).
46. K. M. Leung and Y. F. Liu, Photon band structures - The plane-wave method, *Phys. Rev. B* **41**, 10188-10190 (1990).
47. M. S. Thijssen, R. Sprik, J. Wijnhoven, M. Megens, T. Narayanan, A. Lagendijk, and W. L. Vos, Inhibited light propagation and broadband reflection in photonic air-sphere crystals, *Phys. Rev. Lett.* **83**, 2730-2733 (1999).
48. Y. A. Vlasov, M. Deutsch, and D. J. Norris, Single-domain spectroscopy of self-assembled photonic crystals, *Appl. Phys. Lett.* **76**, 1627-1629 (2000).
49. J. F. Bertone, P. Jiang, K. S. Hwang, D. M. Mittleman, and V. L. Colvin, Thickness dependence of the optical properties of ordered silica-air and air-polymer photonic crystals, *Phys. Rev. Lett.* **83**, 300-303 (1999).
50. K. P. Velikov, A. Moroz, and A. van Blaaderen, Photonic crystals of core-shell colloidal particles, *Appl. Phys. Lett.* **80**, 49-51 (2002).
51. W. L. Vos and H. M. van Driel, Higher order Bragg diffraction by strongly photonic fcc crystals: onset of a photonic bandgap, *Phys. Lett. A* **272**, 101-106 (2000).
52. W. M. Robertson, G. Arjavalingam, R. D. Meade, K. D. Brommer, A. M. Rappe, and J. D. Joannopoulos, Measurement of photonic band-structure in a 2-dimensional periodic dielectric array, *Phys. Rev. Lett.* **68**, 2023-2026 (1992).
53. K. Sakoda, Group-theoretical classification of eigenmodes in three-dimensional photonic lattices, *Phys. Rev. B* **55**, 15345-15348 (1997).
54. Y. A. Vlasov, X. Z. Bo, J. C. Sturm, and D. J. Norris, On-chip natural assembly of silicon photonic bandgap crystals, *Nature* **414**, 289-293 (2001).
55. P. Pieranski, Colloidal crystals, *Contemp. Phys.* **24**, 25-73 (1983).
56. T. Yoshiyama, I. Sogami, and N. Ise, Kossel line analysis on colloidal crystals in semidilute aqueous solutions, *Phys. Rev. Lett.* **53**, 2153-2156 (1984).
57. T. Yoshiyama and I. S. Sogami, Kossel images as direct manifestations of the gap structure of the dispersion surface for colloidal crystals, *Phys. Rev. Lett.* **56**, 1609-1612 (1986).
58. R. D. Pradhan, J. A. Bloodgood, and G. H. Watson, Photonic band structure of bcc colloidal crystals, *Phys. Rev. B* **55**, 9503-9507 (1997).

59. S. John and J. Wang, Quantum electrodynamics near a photonic band-gap - Photon bound-states and dressed atoms, *Phys. Rev. Lett.* **64**, 2418-2421 (1990).
60. S. John and J. Wang, Quantum optics of localized light in a photonic band-gap, *Phys. Rev. B* **43**, 12772-12789 (1991).
61. Y. A. Vlasov, V. N. Astratov, O. Z. Karimov, A. A. Kaplyanskii, V. N. Bogomolov, and A. V. Prokofiev, Existence of a photonic pseudogap for visible light in synthetic opals, *Phys. Rev. B* **55**, 13357-13360 (1997).
62. V. N. Bogomolov, S. V. Gaponenko, I. N. Germanenko, A. M. Kapitonov, E. P. Petrov, N. V. Gaponenko, A. V. Prokofiev, A. N. Ponyavina, N. I. Silvanovich, and S. M. Samoilovich, Photonic band gap phenomenon and optical properties of artificial opals, *Phys. Rev. E* **55**, 7619-7625 (1997).
63. S. G. Romanov, A. V. Fokin, V. I. Alperovich, N. P. Johnson, and R. M. De La Rue, The effect of the photonic stop-band upon the photoluminescence of CdS in opal, *Phys. Status Solidi A-Appl. Res.* **164**, 169-173 (1997).
64. S. G. Romanov, A. V. Fokin, and R. M. De La Rue, Anisotropic photoluminescence in incomplete three-dimensional photonic band-gap environments, *Appl. Phys. Lett.* **74**, 1821-1823 (1999).
65. T. Yamasaki and T. Tsutsui, Spontaneous emission from fluorescent molecules embedded in photonic crystals consisting of polystyrene microspheres, *Appl. Phys. Lett.* **72**, 1957-1959 (1998).
66. A. Blanco, C. Lopez, R. Mayoral, H. Miguez, F. Meseguer, A. Mifsud, and J. Herrero, CdS photoluminescence inhibition by a photonic structure, *Appl. Phys. Lett.* **73**, 1781-1783 (1998).
67. M. Megens, J. Wijnhoven, A. Lagendijk, and W. L. Vos, Light sources inside photonic crystals, *J. Opt. Soc. Am. B* **16**, 1403-1408 (1999).
68. S. G. Romanov, A. V. Fokin, and R. M. De La Rue,  $\text{Eu}^{3+}$  emission in an anisotropic photonic band gap environment, *Appl. Phys. Lett.* **76**, 1656-1658 (2000).
69. K. Sumioka, H. Nagahama, and T. Tsutsui, Strong coupling of exciton and photon modes in photonic crystal infiltrated with organic-inorganic layered perovskite, *Appl. Phys. Lett.* **78**, 1328-1330 (2001).
70. A. J. Campillo, J. D. Eversole, and H. B. Lin, Cavity quantum electrodynamic enhancement of stimulated-emission in microdroplets, *Phys. Rev. Lett.* **67**, 437-440 (1991).
71. B. Y. Tong, P. K. John, Y. T. Zhu, Y. S. Liu, S. K. Wong, and W. R. Ware, Fluorescence-lifetime measurements in monodispersed suspensions of polystyrene particles, *J. Opt. Soc. Am. B* **10**, 356-359 (1993).
72. M. J. A. de Dood, L. H. Slooff, A. Polman, A. Moroz, and A. van Blaaderen, Local optical density of states in  $\text{SiO}_2$  spherical microcavities: Theory and experiment, *Phys. Rev. A* **64**, 033807 (2001).
73. M. J. A. de Dood, L. H. Slooff, A. Polman, A. Moroz, and A. van Blaaderen, Modified spontaneous emission in erbium-doped  $\text{SiO}_2$  spherical colloids, *Appl. Phys. Lett.* **79**, 3585-3587 (2001).
74. K. H. Drexhage, Influence of a dielectric interface on fluorescence decay time, *J. Lumines.* **1,2**, 693 (1970).
75. E. Snoeks, A. Lagendijk, and A. Polman, Measuring and modifying the spontaneous emission rate of Erbium near an interface, *Phys. Rev. Lett.* **74**, 2459-2462 (1995).
76. J. Martorell and N. M. Lawandy, Observation of inhibited spontaneous emission in a periodic dielectric structure, *Phys. Rev. Lett.* **65**, 1877-1880 (1990).
77. N. M. Lawandy, Fluorescence-lifetime measurements in monodispersed suspensions of polystyrene particles - Comment, *J. Opt. Soc. Am. B* **10**, 2144-2146 (1993).
78. M. Tomita, K. Ohosumi, and H. Ikari, Enhancement of molecular interactions in strongly scattering dielectric composite optical media, *Phys. Rev. B* **50**, 10369-10372 (1994).
79. E. P. Petrov, V. N. Bogomolov, Kalosha, II, and S. V. Gaponenko, Spontaneous emission of organic molecules embedded in a photonic crystal, *Phys. Rev. Lett.* **81**, 77-80 (1998).
80. Z. Y. Li and Z. Q. Zhang, Weak photonic band gap effect on the fluorescence lifetime in three-dimensional colloidal photonic crystals, *Phys. Rev. B* **63**, 125106 (2001).
81. M. Megens, H. P. Schriemer, A. Lagendijk, and W. L. Vos, Comment on "Spontaneous emission of organic molecules embedded in a photonic crystal", *Phys. Rev. Lett.* **83**, 5401-5401 (1999).
82. E. P. Petrov, V. N. Bogomolov, Kalosha, II, and S. V. Gaponenko, Comment on "Spontaneous emission of organic molecules embedded in a photonic crystal" - Reply, *Phys. Rev. Lett.* **83**, 5402-5402 (1999).
83. K. Yoshino, S. B. Lee, S. Tsuchihara, Y. Kawagishi, M. Ozaki, and A. A. Zakhidov, Observation of inhibited spontaneous emission and stimulated emission of rhodamine 6G in polymer replica of synthetic opal, *Appl. Phys. Lett.* **73**, 3506-3508 (1998).
84. S. Y. Lin, J. G. Fleming, E. Chow, J. Bur, K. K. Choi, and A. Goldberg, Enhancement and suppression of thermal emission by a three-dimensional photonic crystal, *Phys. Rev. B* **62**, R2243-R2246 (2000).
85. H. P. Schriemer, H. M. van Driel, A. F. Koenderink, and W. L. Vos, Modified spontaneous emission spectra of laser dye in inverse opal photonic crystals, *Phys. Rev. A* **63**, 011801 (2001).

86. A. F. Koenderink, L. Bechger, H. P. Schriemer, A. Lagendijk, and W. L. Vos, Broadband fivefold reduction of vacuum fluctuations probed by dyes in photonic crystals, *Phys. Rev. Lett.* **88**, 143903 (2002).
87. I. I. Tarhan, M. P. Zinkin, and G. H. Watson, Interferometric technique for the measurement of photonic band structure in colloidal crystals, *Opt. Lett.* **20**, 1571-1573 (1995).
88. B. T. Rosner, G. J. Schneider, and G. H. Watson, Interferometric investigation of photonic band-structure effects in pure and doped colloidal crystals, *J. Opt. Soc. Am. B* **15**, 2654-2659 (1998).
89. A. Imhof, W. L. Vos, R. Sprik, and A. Lagendijk, Large dispersive effects near the band edges of photonic crystals, *Phys. Rev. Lett.* **83**, 2942-2945 (1999).
90. Y. A. Vlasov, S. Petit, G. Klein, B. Honerlage, and C. Hirlimann, Femtosecond measurements of the time of flight of photons in a three-dimensional photonic crystal, *Phys. Rev. E* **60**, 1030-1035 (1999).
91. K. M. Ho, C. T. Chan, C. M. Soukoulis, R. Biswas, and M. Sigalas, Photonic band-gaps in 3-dimensions - New layer-by-layer periodic structures, *Solid State Commun.* **89**, 413-416 (1994).
92. E. Ozbay, A. Abeyta, G. Tuttle, M. Tringides, R. Biswas, C. T. Chan, C. M. Soukoulis, and K. M. Ho, Measurement of a 3-dimensional photonic band-gap in a crystal-structure made of dielectric rods, *Phys. Rev. B* **50**, 1945-1948 (1994).
93. C. C. Cheng and A. Scherer, Fabrication of photonic band-gap crystals, *J. Vac. Sci. Technol. B* **13**, 2696-2700 (1995).
94. C. C. Cheng, A. Scherer, V. Arbet-Engels, and E. Yablonovitch, Lithographic band gap tuning in photonic band gap crystals, *J. Vac. Sci. Technol. B* **14**, 4110-4114 (1996).
95. A. Chelnokov, K. Wang, S. Rowson, P. Garoche, and J. M. Lourtioz, Near-infrared Yablonovite-like photonic crystals by focused- ion-beam etching of macroporous silicon, *Appl. Phys. Lett.* **77**, 2943-2945 (2000).
96. A. Birner, R. B. Wehrspohn, U. M. Gosele, and K. Busch, Silicon-based photonic crystals, *Adv. Mater.* **13**, 377-388 (2001).
97. J. Schilling, F. Muller, S. Matthias, R. B. Wehrspohn, U. Gosele, and K. Busch, Three-dimensional photonic crystals based on macroporous silicon with modulated pore diameter, *Appl. Phys. Lett.* **78**, 1180-1182 (2001).
98. S. Shoji and S. Kawata, Photofabrication of three-dimensional photonic crystals by multibeam laser interference into a photopolymerizable resin, *Appl. Phys. Lett.* **76**, 2668-2670 (2000).
99. M. Campbell, D. N. Sharp, M. T. Harrison, R. G. Denning, and A. J. Turberfield, Fabrication of photonic crystals for the visible spectrum by holographic lithography, *Nature* **404**, 53-56 (2000).
100. Y. Monovoukas and A. P. Gast, The experimental phase-diagram of charged colloidal suspensions, *J. Colloid Interface Sci.* **128**, 533-548 (1989).
101. P. N. Pusey, W. van Megen, P. Bartlett, B. J. Ackerson, J. G. Rarity, and S. M. Underwood, Structure of crystals of hard colloidal spheres, *Phys. Rev. Lett.* **63**, 2753-2756 (1989).
102. N. A. M. Verhaegh, J. S. van Duijneveldt, A. van Blaaderen, and H. N. W. Lekkerkerker, Direct observation of stacking disorder in a colloidal crystal, *J. Chem. Phys.* **102**, 1416-1421 (1995).
103. V. N. Astratov, Y. A. Vlasov, O. Z. Karimov, A. A. Kaplyanskii, Y. G. Musikhin, N. A. Bert, V. N. Bogomolov, and A. V. Prokofiev, Photonic band gaps in 3D ordered fcc silica matrices, *Phys. Lett. A* **222**, 349-353 (1996).
104. S. G. Romanov, N. P. Johnson, A. V. Fokin, V. Y. Butko, H. M. Yates, M. E. Pemble, and C. M. S. Torres, Enhancement of the photonic gap of opal-based three-dimensional gratings, *Appl. Phys. Lett.* **70**, 2091-2093 (1997).
105. H. Miguez, C. Lopez, F. Meseguer, A. Blanco, L. Vazquez, R. Mayoral, M. Ocana, V. Fornes, and A. Mifsud, Photonic crystal properties of packed submicrometric SiO<sub>2</sub> spheres, *Appl. Phys. Lett.* **71**, 1148-1150 (1997).
106. H. Miguez, F. Meseguer, C. Lopez, A. Blanco, J. S. Moya, J. Requena, A. Mifsud, and V. Fornes, Control of the photonic crystal properties of fcc-packed submicrometer SiO<sub>2</sub> spheres by sintering, *Adv. Mater.* **10**, 480-483 (1998).
107. H. Miguez, A. Blanco, F. Meseguer, C. Lopez, H. M. Yates, M. E. Pemble, V. Fornes, and A. Mifsud, Bragg diffraction from indium phosphide infilled fcc silica colloidal crystals, *Phys. Rev. B* **59**, 1563-1566 (1999).
108. S. G. Romanov, T. Maka, C. M. S. Torres, M. Muller, R. Zentel, D. Cassagne, J. Manzaneres-Martinez, and C. Jouanin, Diffraction of light from thin-film polymethylmethacrylate opaline photonic crystals, *Phys. Rev. E* **63**, 056603 (2001).
109. A. Reynolds, F. Lopez-Tejeira, D. Cassagne, F. J. Garcia-Vidal, C. Jouanin, and J. Sanchez-Dehesa, Spectral properties of opal-based photonic crystals having a silica matrix, *Phys. Rev. B* **60**, 114221-11426 (1999).
110. R. Biswas, M. M. Sigalas, G. Subramania, and K. M. Ho, Photonic band gaps in colloidal systems, *Phys. Rev. B* **57**, 3701-3705 (1998).

111. R. Biswas, M. M. Sigalas, G. Subramania, C. M. Soukoulis, and K. M. Ho, Photonic band gaps of porous solids, *Phys. Rev. B* **61**, 4549-4553 (2000).
112. A. Imhof and D. J. Pine, Ordered macroporous materials by emulsion templating, *Nature* **389**, 948-951 (1997).
113. A. Imhof and D. J. Pine, Uniform macroporous ceramics and plastics by emulsion templating, *Adv. Mater.* **10**, 697-700 (1998).
114. O. D. Velev, T. A. Jede, R. F. Lobo, and A. M. Lenhoff, Porous silica via colloidal crystallization, *Nature* **389**, 447-448 (1997).
115. O. D. Velev, T. A. Jede, R. F. Lobo, and A. M. Lenhoff, Microstructured porous silica obtained via colloidal crystal templates, *Chem. Mater.* **10**, 3597-3602 (1998).
116. B. T. Holland, C. F. Blanford, and A. Stein, Synthesis of macroporous minerals with highly ordered three-dimensional arrays of spheroidal voids, *Science* **281**, 538-540 (1998).
117. B. T. Holland, C. F. Blanford, T. Do, and A. Stein, Synthesis of highly ordered, three-dimensional, macroporous structures of amorphous or crystalline inorganic oxides, phosphates, and hybrid composites, *Chem. Mater.* **11**, 795-805 (1999).
118. J. E. G. J. Wijnhoven and W. L. Vos, Preparation of photonic crystals made of air spheres in titania, *Science* **281**, 802-804 (1998).
119. C. J. Brinker and G. W. Scherer, *Sol-Gel Science* (Academic, San Diego, 1990).
120. A. Imhof and D. J. Pine, in *Recent Advances in Catalytic Materials*, edited by N. M. Rodriguez, S. L. Soled and J. Hrbek (Materials Research Society, Boston, 1997), Vol. 497, p. 167-172.
121. M. Antonietti, B. Berton, C. Goeltner, and H. P. Hentze, Synthesis of mesoporous silica with large pores and bimodal size distribution by templating of polymer lattices, *Adv. Mater.* **10**, 154-159 (1998).
122. J. S. Yin and Z. L. Wang, Template-assisted self-assembly and cobalt doping of ordered mesoporous titania nanostructures, *Adv. Mater.* **11**, 469-472 (1999).
123. A. Richel, N. P. Johnson, and D. W. McComb, Observation of Bragg reflection in photonic crystals synthesized from air spheres in a titania matrix, *Appl. Phys. Lett.* **76**, 1816-1818 (2000).
124. J. Wijnhoven, L. Bechger, and W. L. Vos, Fabrication and characterization of large macroporous photonic crystals in titania, *Chem. Mater.* **13**, 4486-4499 (2001).
125. M. Muller, R. Zentel, T. Maka, S. G. Romanov, and C. M. Sotomayor Torres, Photonic crystal films with high refractive index contrast, *Adv. Mater.* **12**, 1499-1503 (2000).
126. S. A. Johnson, P. J. Ollivier, and T. E. Mallouk, Ordered mesoporous polymers of tunable pore size from colloidal silica templates, *Science* **283**, 963-965 (1999).
127. A. A. Zakhidov, R. H. Baughman, Z. Iqbal, C. Cui, I. Khayrullin, S. O. Dantas, J. Marti, and V. G. Ralchenko, Carbon structures with three-dimensional periodicity at optical wavelengths, *Science* **282**, 897-901 (1998).
128. Y. A. Vlasov, N. Yao, and D. J. Norris, Synthesis of photonic crystals for optical wavelengths from semiconductor quantum dots, *Adv. Mater.* **11**, 165-169 (1999).
129. P. Jiang, K. S. Hwang, D. M. Mittleman, J. F. Bertone, and V. L. Colvin, Template-directed preparation of macroporous polymers with oriented and crystalline arrays of voids, *J. Am. Chem. Soc.* **121**, 11630-11637 (1999).
130. A. Blanco, E. Chomski, S. Grabtchak, M. Ibisate, S. John, S. W. Leonard, C. López, F. Meseguer, H. Míguez, J. P. Mondia, G. A. Ozin, O. Toader, H. M. van Driel, Large-scale synthesis of a silicon photonic crystal with a complete three-dimensional bandgap near 1.5 micrometers, *Nature* **405**, 437-440 (2000).
131. G. Subramanian, V. N. Manoharan, J. D. Thorne, and D. J. Pine, Ordered macroporous materials by colloidal assembly: A possible route to photonic bandgap materials, *Adv. Mater.* **11**, 1261-1265 (1999).
132. G. Subramania, K. Constant, R. Biswas, M. M. Sigalas, and K. M. Ho, Optical photonic crystals fabricated from colloidal systems, *Appl. Phys. Lett.* **74**, 3933-3935 (1999).
133. G. Subramania, R. Biswas, K. Constant, M. M. Sigalas, and K. M. Ho, Structural characterization of thin film photonic crystals, *Phys. Rev. B* **63**, 235111 (2001).
134. Q. B. Meng, Z. Z. Gu, O. Sato, and A. Fujishima, Fabrication of highly ordered porous structures, *Appl. Phys. Lett.* **77**, 4313-4315 (2000).
135. O. D. Velev, P. M. Tessier, A. M. Lenhoff, and E. W. Kaler, A class of porous metallic nanostructures, *Nature* **401**, 548-548 (1999).
136. P. Tessier, O. D. Velev, A. T. Kalambur, A. M. Lenhoff, J. F. Rabolt, and E. W. Kaler, Structured metallic films for optical and spectroscopic applications via colloidal crystal templating, *Adv. Mater.* **13**, 396-400 (2001).
137. S. H. Park and Y. Xia, Fabrication of three-dimensional macroporous membranes with assemblies of microspheres as templates, *Chem. Mater.* **10**, 1745-1747 (1998).
138. M. Deutsch, Y. A. Vlasov, and D. J. Norris, Conjugated-polymer photonic crystals, *Adv. Mater.* **12**, 1176-1180 (2000).

139. H. Miguez, F. Meseguer, C. Lopez-Tejiera, and J. Sanchez-Dehesa, Synthesis and photonic bandgap characterization of polymer inverse opals, *Adv. Mater.* **13**, 393-396 (2001).
140. H. W. Yan, C. F. Blanford, B. T. Holland, W. H. Smyrl, and A. Stein, General synthesis of periodic macroporous solids by templated salt precipitation and chemical conversion, *Chem. Mater.* **12**, 1134-1141 (2000).
141. H. Yan, C. F. Blanford, B. T. Holland, M. Parent, W. H. Smyrl, and A. Stein, A chemical synthesis of periodic macroporous NiO and metallic Ni, *Adv. Mater.* **11**, 1003-1006 (1999).
142. P. V. Braun and P. Wiltzius, Electrochemically grown photonic crystals, *Nature* **402**, 603-604 (1999).
143. P. V. Braun and P. Wiltzius, Electrochemical fabrication of 3D microperiodic porous materials, *Adv. Mater.* **13**, 482-485 (2001).
144. J. Wijnhoven, S. J. M. Zevenhuizen, M. A. Hendriks, D. Vanmackelbergh, J. J. Kelly, and W. L. Vos, Electrochemical assembly of ordered macropores in gold, *Adv. Mater.* **12**, 888-890 (2000).
145. M. C. Netti, S. Coyle, J. J. Baumberg, M. A. Ghanem, P. R. Birkin, P. N. Bartlett, and D. M. Whittaker, Confined surface plasmons in gold photonic nanocavities, *Adv. Mater.* **13**, 1368-1370 (2001).
146. P. Jiang, J. Cizeron, J. F. Bertone, and V. L. Colvin, Preparation of macroporous metal films from colloidal crystals, *J. Am. Chem. Soc.* **121**, 7957-7958 (1999).
147. N. Eradat, J. D. Huang, Z. V. Vardeny, A. A. Zakhidov, I. Khayrullin, I. Udod, and R. H. Baughman, Optical studies of metal-infiltrated opal photonic crystals, *Synthetic Metals* **116**, 501-504 (2001).
148. H. Miguez, E. Chomski, F. Garcia-Santamaria, M. Ibasate, S. John, C. Lopez, F. Meseguer, J. P. Mondia, G. A. Ozin, O. Toader, and H. M. van Driel, Photonic bandgap engineering in germanium inverse opals by chemical vapor deposition, *Adv. Mater.* **13**, 1634-1637 (2001).
149. N. D. Denkov, O. D. Velev, P. A. Kralchevsky, I. B. Ivanov, H. Yoshimura, and K. Nagayama, Mechanism of formation of 2-dimensional crystals from latex particles on substrates, *Langmuir* **8**, 3183-3190 (1992).
150. N. D. Denkov, O. D. Velev, P. A. Kralchevsky, I. B. Ivanov, H. Yoshimura, and K. Nagayama, 2-Dimensional crystallization, *Nature* **361**, 26-26 (1993).
151. P. Jiang, J. F. Bertone, K. S. Hwang, and V. L. Colvin, Single-crystal colloidal multilayers of controlled thickness, *Chem. Mater.* **11**, 2132-2140 (1999).
152. M. E. Turner, T. J. Trentler, and V. L. Colvin, Thin films of macroporous metal oxides, *Adv. Mater.* **13**, 180-183 (2001).
153. S. H. Park, D. Qin, and Y. Xia, Crystallization of mesoscale particles over large areas, *Adv. Mater.* **10**, 1028-1032 (1998).
154. S. H. Park and Y. Xia, Assembly of mesoscale particles over large areas and its application in fabricating tunable optical filters, *Langmuir* **15**, 266-273 (1999).
155. B. Gates, D. Qin, and Y. Xia, Assembly of nanoparticles into opaline structures over large areas, *Adv. Mater.* **11**, 466-469 (1999).
156. B. T. Mayers, B. Gates, and Y. Xia, Crystallization of mesoscopic colloids into 3D opaline lattices in packing cells fabricated by replica molding, *Adv. Mater.* **12**, 1629-1632 (2000).
157. R. M. Amos, J. G. Rarity, P. R. Tapster, T. J. Shepherd, and S. C. Kitson, Fabrication of large-area face-centered-cubic hard-sphere colloidal crystals by shear alignment, *Phys. Rev. E* **61**, 2929-2935 (2000).
158. M. Trau, D. A. Saville, and I. A. Aksay, Field-induced layering of colloidal crystals, *Science* **272**, 706-709 (1996).
159. M. Holgado, *et al.*, Electrophoretic deposition to control artificial opal growth, *Langmuir* **15**, 4701-4704 (1999).
160. R. C. Hayward, D. A. Saville, and I. A. Aksay, Electrophoretic assembly of colloidal crystals with optically tunable micropatterns, *Nature* **404**, 56-59 (2000).
161. A. L. Rogach, N. A. Kotov, D. S. Koktysh, J. W. Ostrander, and G. A. Ragoisha, Electrophoretic deposition of latex-based 3D colloidal photonic crystals: A technique for rapid production of high-quality opals, *Chem. Mater.* **12**, 2721-2726 (2000).
162. A. van Blaaderen, R. Ruel, and P. Wiltzius, Template-directed colloidal crystallization, *Nature* **385**, 321-324 (1997).
163. A. van Blaaderen and P. Wiltzius, Growing large, well-oriented colloidal crystals, *Adv. Mater.* **9**, 833 (1997).
164. P. V. Braun, R. W. Zehner, C. A. White, M. K. Weldon, C. Kloc, S. S. Patel, and P. Wiltzius, Epitaxial growth of high dielectric contrast three-dimensional photonic crystals, *Adv. Mater.* **13**, 721-724 (2001).
165. A. van Blaaderen *et al.*, in *Photonic Crystals and Light Localization in the 21st Century*, edited by C. M. Soukoulis (Kluwer Academic, Dordrecht, 2001).
166. Y. D. Yin and Y. N. Xia, Growth of large colloidal crystals with their (100) planes orientated parallel to the surfaces of supporting substrates, *Adv. Mater.* **14**, 605-608 (2002).
167. S. Hachisu and S. Yoshimura, *Nature* **283**, 188 (1980).

168. P. Bartlett, R. H. Ottewill, and P. N. Pusey, Superlattice formation in binary mixtures of hard-sphere colloids, *Phys. Rev. Lett.* **68**, 3801-3804 (1992).
169. K. P. Velikov, C. G. Christova, R. P. A. Dullens, and A. van Blaaderen, Layer-by-layer growth of binary colloidal crystals, *Science* **296**, 106-109 (2002).
170. U. Dassanayake, S. Fraden, and A. van Blaaderen, Structure of electrorheological fluids, *J. Chem. Phys.* **112**, 3851-3858 (2000).
171. F. García-Santamaría, C. López, F. Meseguer, F. López-Tejiera, J. Sánchez-Dehesa, and H. T. Miyazaki, Opal-like photonic crystal with diamond lattice, *Appl. Phys. Lett.* **79**, 2309-2311 (2001).
172. H. T. Miyazaki, H. Miyazaki, K. Ohtaka, and T. Sato, Photonic band in two-dimensional lattices of micrometer-sized spheres mechanically arranged under a scanning electron microscope, *J. Appl. Phys.* **87**, 7152-7158 (2000).
173. R. D. Pradhan, Tarhan, II, and G. H. Watson, Impurity modes in the optical stop bands of doped colloidal crystals, *Phys. Rev. B* **54**, 13721-13726 (1996).
174. Y. A. Vlasov, M. A. Kaliteevski, and V. V. Nikolaev, Different regimes of light localization in a disordered photonic crystal, *Phys. Rev. B* **60**, 1555-1562 (1999).
175. Y. A. Vlasov, V. N. Astratov, A. V. Baryshev, A. A. Kaplyanski, O. Z. Karimov, and M. F. Limonov, Manifestation of intrinsic defects in optical properties of self-organized opal photonic crystals, *Phys. Rev. E* **61**, 5784-5793 (2000).
176. A. F. Koenderink, M. Megens, G. van Soest, W. L. Vos, and A. Lagendijk, Enhanced backscattering from photonic crystals, *Phys. Lett. A* **268**, 104-111 (2000).
177. J. Huang, N. Eradat, M. E. Raikh, Z. V. Vardeny, A. A. Zakhidov, and R. H. Baughman, Anomalous coherent backscattering of light from opal photonic crystals, *Phys. Rev. Lett.* **86**, 4815-4818 (2001).
178. Z. Y. Li and Z. Q. Zhang, Fragility of photonic band gaps in inverse-opal photonic crystals, *Phys. Rev. B* **62**, 1516-1519 (2000).
179. Z. Y. Li and Z. Q. Zhang, Photonic bandgaps in disordered inverse-opal photonic crystals, *Adv. Mater.* **13**, 433-436 (2001).
180. S. H. Fan, P. R. Villeneuve, and J. D. Joannopoulos, Theoretical Investigation of Fabrication-Related Disorder On the Properties of Photonic Crystals, *J. Appl. Phys.* **78**, 1415-1418 (1995).
181. A. Chutinan and S. Noda, Effects of structural fluctuations on the photonic bandgap during fabrication of a photonic crystal, *J. Opt. Soc. Am. B* **16**, 240-244 (1999).
182. M. M. Sigalas, C. M. Soukoulis, C. T. Chan, R. Biswas, and K. M. Ho, Effect of disorder on photonic band gaps, *Phys. Rev. B* **59**, 12767-12770 (1999).
183. V. Yannopapas, N. Stefanou, and A. Modinos, Effect of stacking faults on the optical properties of inverted opals, *Phys. Rev. Lett.* **86**, 4811-4814 (2001).
184. F. Caruso, Nanoengineering of particle surfaces, *Adv. Mater.* **13**, 11-22 (2001).
185. A. van Blaaderen and A. Vrij, Synthesis and characterization of colloidal dispersions of fluorescent, monodisperse silica spheres, *Langmuir* **8**, 2921-2931 (1992).
186. A. Rogach, A. Susa, F. Caruso, G. Sukhorukov, A. Kornowski, S. Kershaw, H. Mohwald, A. Eychmuller, and H. Weller, Nano- and microengineering: Three-dimensional colloidal photonic crystals prepared from submicrometer-sized polystyrene latex spheres pre-coated with luminescent polyelectrolyte/nanocrystal shells, *Adv. Mater.* **12**, 333-337 (2000).
187. P. Jiang, J. F. Bertone, and V. L. Colvin, A lost-wax approach to monodisperse colloids and their crystals, *Science* **291**, 453-457 (2001).
188. R. Rengarajan, P. Jiang, D. C. Larrabee, V. L. Colvin, and D. M. Mittleman, Colloidal photonic superlattices, *Phys. Rev. B* **64**, 205103 (2001).
189. A. Imhof, Preparation and characterization of titania-coated polystyrene spheres and hollow titania shells, *Langmuir* **17**, 3579-3585 (2001).
190. G. R. Yi and S. M. Yang, Bandgap engineering of face-centered cubic photonic crystals made of hollow spheres, *J. Opt. Soc. Am. B* **18**, 1156-1160 (2001).
191. A. Moroz, Three-dimensional complete photonic-band-gap structures in the visible, *Phys. Rev. Lett.* **83**, 5274-5277 (1999).
192. A. Moroz, Photonic crystals of coated metallic spheres, *Europhys. Lett.* **50**, 466-472 (2000).
193. W. Y. Zhang, X. Y. Lei, Z. L. Wang, D. G. Zheng, W. Y. Tam, C. T. Chan, and P. Sheng, Robust photonic band gap from tunable scatterers, *Phys. Rev. Lett.* **84**, 2853-2856 (2000).
194. Z. L. Wang, C. T. Chan, W. Y. Zhang, N. B. Ming, and P. Sheng, Three-dimensional self-assembly of metal nanoparticles: Possible photonic crystal with a complete gap below the plasma frequency, *Phys. Rev. B* **64**, 113108 (2001).
195. S. J. Oldenburg, R. D. Averitt, S. L. Westcott, and N. J. Halas, Nanoengineering of optical resonances, *Chem. Phys. Lett.* **288**, 243-247 (1998).

196. C. Graf and A. van Blaaderen, Metallodielectric colloidal core-shell particles for photonic applications, *Langmuir* **18**, 524-534 (2002).
197. J. B. Jackson and N. J. Halas, Silver nanoshells: Variations in morphologies and optical properties, *J. Phys. Chem. B* **105**, 2743-2746 (2001).
198. A. B. R. Mayer, W. Grebner, and R. Wannemacher, Preparation of silver-latex composites, *J. Phys. Chem. B* **104**, 7278-7285 (2000).
199. S. J. Oldenburg, G. D. Hale, J. B. Jackson, and N. J. Halas, Light scattering from dipole and quadrupole nanoshell antennas, *Appl. Phys. Lett.* **75**, 1063-1065 (1999).
200. S. J. Oldenburg, S. L. Westcott, R. D. Averitt, and N. J. Halas, Surface enhanced Raman scattering in the near infrared using metal nanoshell substrates, *J. Chem. Phys.* **111**, 4729-4735 (1999).
201. M. V. Artemyev, U. Woggon, R. Wannemacher, H. Jaschinski, and W. Langbein, Light trapped in a photonic dot: Microspheres act as a cavity for quantum dot emission, *Nano Letters* **1**, 309-314 (2001).
202. J. W. Haus, H. S. Sozuer, and R. Inguva, Photonic bands - Ellipsoidal dielectric atoms in an f.c.c. lattice, *J. Mod. Opt.* **39**, 1991-2005 (1992).
203. Z. Y. Li, J. Wang, and B. Y. Gu, Creation of partial band gaps in anisotropic photonic-band-gap structures, *Phys. Rev. B* **58**, 3721-3729 (1998).
204. E. Matijevic, Preparation and properties of uniform size colloids, *Chem. Mater.* **5**, 412-426 (1993).
205. Y. Lu, Y. D. Yin, and Y. N. Xia, Three-dimensional photonic crystals with non-spherical colloids as building blocks, *Adv. Mater.* **13**, 415-420 (2001).
206. E. Snoeks, A. van Blaaderen, T. van Dillen, C. M. van Kats, M. L. Brongersma, and A. Polman, Colloidal ellipsoids with continuously variable shape, *Adv. Mater.* **12**, 1511-1514 (2000).
207. E. Snoeks, A. van Blaaderen, T. van Dillen, C. M. van Kats, K. Velikov, M. L. Brongersma, and A. Polman, Colloidal assemblies modified by ion irradiation, *Nuclear Instruments & Methods in Physics Research Section B* **178**, 62-68 (2001).
208. W. M. Lee, S. A. Pruzinsky, and P. V. Braun, Multi-photon polymerization of waveguide structures within three-dimensional photonic crystals, *Adv. Mater.* **14**, 271-274 (2002).
209. K. Yoshino, Y. Shimoda, Y. Kawagishi, K. Nakayama, and M. Ozaki, Temperature tuning of the stop band in transmission spectra of liquid-crystal infiltrated synthetic opal as tunable photonic crystal, *Appl. Phys. Lett.* **75**, 932-934 (1999).